CONTENTS

METAL ALLOYING WITH NITROGEN
FROM GAS PHASE IN ESR PROCESS

A.D. RYABTSEV, A.A. TROYANSKY, E.L. KORZUN, V.Yu. MASTEPAN and **M.V. SAMBORSKY**

Donetsk National Technical University, Donetsk, Ukraine

Using a thermodynamic analysis an attempt was made to evaluate the feasibility of metal nitriding from a gas phase during the electroslag remelting (ESR). It was shown experimentally that in use of slags of Ca–CaF$_2$ system and atmosphere of nitrogen in chamber-type ESR units the necessary conditions are created for transition of nitrogen to metal in the amounts sufficient for nitriding.

Key words: *nitriding, electroslag remelting, chamber furnace, metal calcium*

The use of nitrogen as alloying element is well-known and realized by manufacturers for producing steel designed, first of all, for operation under the complex conditions. However, the mechanism of nitrogen injection into a steel as compared with mechanisms of injection of other alloying elements has some specific features and presents until now a great interest from the point of view of study of laws of nitrogen behaviour and development of a comparatively inexpensive method of steel production with a guaranteed level of the nitrogen content.

The basic methods of nitrogen injection into metal are connected with

• use of materials having a high content of a dissolved nitrogen,

• nitrogen compounds easily decomposing at temperatures of the metallurgical process,

• activation of molecular nitrogen and its dissolution in molten metal.

Disadvantages of the first two methods are the necessity in production of special ferroalloys or chemical compositions, instability of assimilation of nitrogen from them in the process of alloying and rather high non-uniformity of nitrogen content in the ready metal.

Evidently, it is more rational from the ecological and economical aspects to use a gaseous nitrogen for the metal alloying. However, the difficulties occurring due to energy consumption for activation of intermolecular bonds limit the wide spreading of alloying with nitrogen from the gas phase. Works on mastering methods of metal alloying with nitrogen from the gas phase are carried out intensively for several decades both in our country and abroad [1–7].

It is possible to alloy metal with a gaseous nitrogen both in liquid and solid aggregate states. Nitriding of solid metal is used for products having small sections or produced by the methods of powder metallurgy [7–9]. Technologies of alloying with nitrogen from the gas phase of molten metal are more widely used. They can be classified by a value of the gas phase pressure in units in which the alloying processes are proceeding:

• at pressure below atmospheric — vacuum-arc remelting (VAR) [10] and plasma-arc remelting (PAR) [1, 2, 11, 12];

• at atmospheric pressure — blowing of molten metal in a ladle [7], vacuum- and gas-oxygen decarburization of metal [7, 13], plasma-arc remelting [1, 2] and arc slag remelting (ASR) [6];

• at increased pressure (up to 12 MPa) — pressure pouring [3], plasma-arc remelting [1, 2], electroslag heating of molten metal under pressure (ESHP) [4], arc slag remelting under pressure (ASRP) [5] and induction melting under pressure [3, 14, 15].

Analysis of technology of methods of alloying with a gaseous nitrogen shows that to produce steels with a level of nitrogen content to 0.03 % the processes, proceeding in open units: blowing in a ladle, vacuum- and gas-oxygen decarburization, are quite acceptable. Technologies and units used for producing high-nitrogen and superhigh-nitrogen steels are operating usually at gas pressures which differ from the atmospheric pressure. In addition, all the methods of producing high-nitrogen steels are characterized by a high energy consumption, complexity of equipment, especially those realized at higher pressures, and also by a need of preliminary melting of initial metal with a required final chemical composition except nitrogen.

Method of VAR for production of high-nitrogen and superhigh-nitrogen steels did not find a wide spreading due to difficulties connected with a stabilization of arc discharge at working pressures 1–90 kPa and low output of efficient quality metal, typical of the VAR. Method of PAR, in spite of numerous advantages, do not find a wide spreading in the production of the above-mentioned steels due to complexity of equipment and high expenses for production. Method ASR, being less energy- and resources-consuming process, requires the preliminary preparation of a consumable electrode, as the technology of alloying with a gaseous nitrogen envisages in this case the nitrogen blowing into the arc region

through a cavity in the electrode that makes the final production more expensive.

The present work is aimed at testing the feasibility of producing steels alloyed with nitrogen from the gas phase at the pressure in the unit equal to the atmospheric pressure.

Laws of nitrogen behaviour in steel-making processes using a slag. Activity of components α_i in a slag oxide phase depends not only on concentration of component c_i, but also on a partial pressure of oxygen P_{O_2} over the slag melt [16]. Concentration and activity of the i-th component in slag are combined in the following expression:

$$c_i = k' \, a_i \, P_{O_2}^{\frac{v_i}{4}} , \qquad (1)$$

where k' is the constant of equilibrium reaction; v_i is the valency of the i-th component in slag.

This fact, confirmed experimentally [16–18] in real metallurgical systems, leads to the appearance of «pumping» effect [19]. Let us consider the «pumping» effect as regards to nitrogen on definite example. It is known that slag, contacting the furnace atmosphere ($P = 101325$ Pa and $P_{O_2} = 21278.25$ Pa), does not dissolve nitrogen in principle. Being in contact with metal the slag layer is deoxidized ([O] ≈ 0.1 % and $P_{O_2} \approx 1.013 \cdot 10^{-3}$ Pa) and dissolves a noticeable amount of nitrogen.

At convective movement the separate slag portions appear in turn in the regions of a lower and increased oxidation, absorbing nitrogen near the metal and exhausting it into atmosphere (Figure).

Slag stirring plays an active role in the operation of the nitrogen «pump», increasing abruptly its efficiency. However, even in the absence of stirring the «pumping» effect should exist and be governed by the same laws. It follows from the above-said, that a real nitrogen concentration in metal is always lower, while that of hydrogen is higher than the equilibrium concentration with a furnace atmosphere. This deviation can reach high values:

$$[N]_{min} = [N]_{eq} \cdot \left(\frac{P_{O_2}^I}{P_{O_2}^{II}} \right)^{-\frac{3}{4}} . \qquad (2)$$

The above law of nitrogen behaviour have been confirmed in practice. The nitrogen content is more than 10 times lower than equilibrium content in all the open steel-making units and even in arc electric furnaces where the intensive metal saturation with nitrogen in the arc regions takes place. At holding under slag the hydrogen content in metal is increased, while the nitrogen content is decreased [20–23].

Consequently, to alloy metal with nitrogen from the gas phase it is necessary to provide: the use of molten and mobile (stirring) slag; the presence of reduction atmosphere near gas–slag interface; the presence of gradient of slag oxidability directed from slag–metal in-
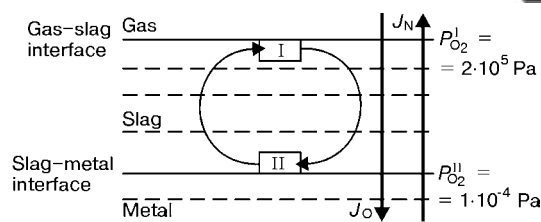

Diagram of appearance of «pumping» effect in oxide slags (J_O — oxygen flow, J_N — nitrogen flow)

terface to gas–slag interface ($P_{O_2}^I < P_{O_2}^{II}$), here, the higher this gradient the higher the motive force of the alloying process.

To realize all the above-listed conditions, an ESR in a chamber furnace was suggested using active Ca-containing slags [24] with a replacement of neutral gas atmosphere by N-containing non-oxidizing atmosphere. This method satisfies the above requirements of metal alloying with a gaseous nitrogen using a «pumping» effect, namely slag is used; a low chemical potential of oxygen due to presence of calcium in slag and its active evaporation is created in a small gas layer over the slag; slag is stirring intensively owing to magnetohydrodynamic effects in the furnace pool. Presence of metal calcium in slag promotes an abrupt decrease of sulphur content in metal whose presence influences negatively on saturation of iron melts with nitrogen [25].

To verify the above-given considerations several basic or comparative experiments of producing ESR ingots were performed using: slag ANF-1P, fluoride slags with creation of an oxygen flow during remelting directed from metal to furnace atmosphere due to oxidation of hydrogen added in the form of thermosplitting graphite material (TSGM) at the slag–gas interface; fluoride slags with the creation of oxygen flow during remelting directed from metal to furnace atmosphere due to calcium oxidation at the slag–gas interface.

Procedure of conductance of experiments. Remelting of 45 mm diameter electrodes from St.50 (0.3 wt.% C, Fe — balance) was realized in a chamber furnace, manufactured on the base of unit A-550 [26], into a 90 mm diameter mould. Electrical conditions of remelting were as follows: 1.8–2.0 kA current, 40 V voltage. Commercial flux ANF-1P and calcium fluoride OSCh-5-2 (TU-6-09-2412–72) were used as main components of slag, while metal calcium of 99.5 % purity and TSGM were used as additional components [27]. Additions were added to the flux by mixing an adding component to the initial main component before the melting beginning. To create the furnace atmosphere the following elements were used: gaseous argon with a volume share of argon ≥ 99.992, oxygen ≤ 0.0007, nitrogen ≤ 0.005 %; gaseous nitrogen with a volume share of nitrogen ≥ 99.99, oxygen ≤ 0.0007, argon ≤ 005 %. Gas pressure in furnace chamber was maintained at the 101 kPa level.

Transverse 10 mm thick templets were cut from the produced ingots at 15 and 90 mm height from their bottom part and then the chips were taken from

Melting No.	Composition of initial flux components, %	Furnace atmosphere	Content of elements in metal, wt.%		
			N	O	S
	Initial metal		0.0061	0.0186	0.0143
1	ANF-1P — 100	Air	0.0075 / 0.0066	– / 0.0161	0.0046 / 0.0053
2	ANF-1P — 89.3 Ca — 6.0 TSGM — 4.7	Same	0.0134 / 0.0088	– / 0.0183	0.0039 / 0.0067
3	CaF$_2$ — 93.75 Ca — 6.25	Argon	0.0023 / 0.0044	– / 0.0071	0.0025 / 0.0019
4	CaF$_2$ — 93.75 Ca — 6.25	Nitrogen	0.0182 / 0.0265	– / 0.0094	0.0030 / 0.0026
5	CaF$_2$ — 100	Same	0.0127 / 0.0090	– / 0.0105	0.0080 / 0.0145
6	CaF$_2$ — 97.4 TSGM — 2.6	»	0.0080 / 0.0071	– / 0.0179	0.0096 / 0.0116

Note. Above the line the element content in sample taken at 15 mm level from the ingot bottom is given, under the line — the same at 90 mm level from the ingot bottom.

them to analyze the sulphur and nitrogen content in metal. To determine the oxygen content the standard samples were manufactured from the templet axial part. Content of gases was examined by a standard procedure in LECO units TC-300 and EF-300. Error in determination of nitrogen and oxygen content was $1 \cdot 10^{-3}$ wt.%. Sulphur content was evaluated by the method of infrared spectroscopy using a standard procedure in LECO unit CS-200, the error in determination was $2 \cdot 10^{-4}$ wt.%. Each determination was made not less than 3 times. Results of chemical analysis of metal after ESR are given in the Table.

Discussion of results. During remelting in air (melt No.1) the nitrogen content in steel is not almost changed, though the oxygen content is decreased that is evidently due in the open process to the assimilation of oxide inclusions by a slag . At similar remelting in nitrogen atmosphere (melt No.5) a small increase in its content in the remelted metal is observed.

Remelting under the Ca-containing slag in argon atmosphere (melt No.3) leads to an abrupt decrease in content of controllable impurity elements in steel: oxygen, nitrogen and sulphur. In adding metal calcium to slag and in nitrogen remelting the metal is saturated with nitrogen from the gas phase (melt No.4). However, when TSGM is added (melt No.2, 6) the effect of nitrogen «pumping» is not confirmed.

In our opinion, this nitrogen behaviour is explained by the composition of slag system used for remelting: we used a fluoride system, and theoretical considerations were made on the basis of analysis of nitrogen behaviour in oxide slags. It can be assumed with a high probability for the fluoride system or fluoride-oxide systems with a dominating fluoride part similarly to the laws set for oxide phases (expression (1)), that the activity of component in slag depends not only on its concentration, but also on a partial pressure of fluorine over the slag melt:

$$c_i = k' \, a_i \, P_{F_2}^{\frac{v_i}{2}} . \qquad (3)$$

For nitrogen the expression (3) takes a form

$$(N) = k_N \, P_{N_2}^{\frac{1}{2}} \, P_{F_2}^{-\frac{3}{2}} . \qquad (4)$$

To define the direction of fluorine flow in the process of ESR, we calculate the value of an equilibrium partial pressure of fluorine at the slag−gas and metal−slag interfaces. Under conditions of open ESR process using a fluoride slag the equilibrium fluorine pressure at the above-mentioned interfaces is determined by the equilibrium of reaction of formation of calcium fluoride being a slag base:

$$\{Ca\} + \{F_2\} = (CaF_2) . \qquad (5)$$
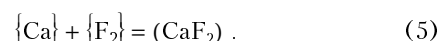
Gibbs energy (J/mol) of equation (5) has the following dependence on temperature [16]:

$$\Delta G_6 = -970000 + 84 \, T . \qquad (6)$$

High values of constant of equilibrium of reaction (6) — $K_6 = 4.6 \cdot 10^{22}$ at 1873 K and $K_6 = 9.1 \cdot 10^{21}$ at 1973 K indicate about very low values of partial pressure of fluorine at both phase interfaces. Absence of a very strong reducer of calcium fluoride both in gas and in metallic phases stipulates the equality of partial pressures of fluorine at the phase interfaces considered.

At TSGM adding to the slag surface the equilibrium of reaction (5) due to carbon fluorides formation is not disturbed:

$$c_{interface} + 2 \, (CaF_2) = \{CF_4\} + \{Ca\} ; \qquad (7)$$

$$\Delta G_7 = 36800 + 67.5 \, T > 0. \qquad (8)$$

Therefore in metal of melts No.2 and 6 the nitrogen content is close to its content in a reference ingot (melt No.1).

When metal calcium is added to the slag composition, we shift artificially the equilibrium of reaction (5) towards the initial substances. Here, it is possible to calculate the fluorine partial pressure over a Ca-containing slag, assuming partial pressure of calcium in the first approximation to be equal to 101325 Pa:

$$K_6 = \frac{a_{(CaF_2)}}{P_{Ca}\,P_{F_2}} \ . \qquad (9)$$

Value of fluorine partial pressure at the gas–slag interface is determined from the following expression:

$$P_{F_2} = \frac{a_{(CaF_2)}}{K_6\,P_{Ca}} = \frac{a_{(CaF_2)}}{\exp\!\left(-\dfrac{\Delta G_6}{RT}\right)P_{Ca}} =$$

$$(10)$$

$$= \frac{1}{\exp\!\left(-\dfrac{\Delta G_6}{RT}\right)} = \exp\!\left(\dfrac{\Delta G_6}{RT}\right).$$

Let us assume the activity of calcium fluoride to be equal to unity and the temperature of slag–gas interface — to 1973 K. Then, the partial pressure of fluorine at the gas–slag interface will be $P_{F_2}^{l} = 1.1 \cdot 10^{-17}$ Pa.

To consider the fluorine behaviour at slag–metal phase interface, let us assume the following: base of the molten metal is iron, concentrations of rest elements are neglected; fluorine solution in molten iron is infinitely diluted.

Taking into account the distribution of calcium, added to the initial flux, between phases of the system, the behaviour of fluorine at slag–metal interface can be described by reaction

$$[Ca]_{Fe} + 2\,[F]_{Fe} = (CaF_2). \qquad (11)$$
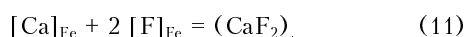
This reaction can be presented as a sum of reaction (5) and the following reactions:

$$Ca = [Ca]_{Fe} ; \qquad (12)$$

$$\Delta G_{10} = 163200 - 58.6\,T\ [19]; \qquad (13)$$

$$\frac{1}{2}F_2 = [F]_{Fe} ; \qquad (14)$$

$$\Delta G_{12} = A + BT. \qquad (15)$$

Taking into account the above-given assumptions, the value of parameter A in formula (15) can be set equal to the value of initial heat of fluorine dissolution in a molten iron which can be estimated using method Miedema [28, 29] by formula

$$\Delta H_F^{\infty} = \frac{2\,V_F^{\frac{2}{3}}\,p}{n_{WS_{Fe}}^{-\frac{1}{3}} + n_{WS_F}^{-\frac{1}{3}}} \times \qquad (16)$$

$$\times \left\{ -(k_{Fe} - k_F)^2 + Q\left(n_{WS_{Fe}}^{\frac{1}{3}} - n_{WS_F}^{\frac{1}{3}}\right)^2 - aR \right\},$$

where $V_F = 14.61$ cm^3/mol is the molar volume of fluorine [30]; $n_{WS_{Fe}} = 5.54$ is the electron density at the boundaries of atomic cell of Wigner–Seitz, conditional units of density [31]; $k_{Fe} = 4.93$ [28] and $k_F = 3$ [30] are the electronegativity of elements, respectively; $p = 14200$ J/mol [28], $Q = 9400$ J/mol and $R = 0$ [29] are the parameters of Miedema's model; a is the coefficient taking into account the aggregate state of solution, for liquid solutions $a = 0.73$ [29].

Value of electronic density at the boundaries of atomic cell of Wigner–Seitz for fluorine was determined by empiric correlation relationship found by Miedema [31]:

$$n_{WS_F} = 8.2 \cdot 10^{-5}\left(\frac{B_i}{V_i}\right)^{\frac{1}{2}}, \qquad (17)$$

where B_i is the volume modulus of compression, kg/cm^2, which is determined from expression [32]

$$B_i = \left(\frac{6.13}{r_s/a_0}\right)^5 \cdot 10^{10}\ (dyn/cm^2) = \left(\frac{6.13}{r_s/a_0}\right)^5 \cdot 10197, \qquad (18)$$

where a_0 is the Bohr radius; r_s is the radius of sphere, whose volume is equal to the volume falling on one electron of conductivity:

$$r_s = \left(\frac{3}{4\,\pi\,n_i}\right)^{\frac{1}{3}}, \qquad (19)$$

where n_i is the density of electron gas in study of element dissolving in a metallic state:

$$n_i = \frac{N_A\,z_i\,\rho_i^{m}}{A_i} , \qquad (20)$$

where $N_A = 6.022 \cdot 10^{23}$ is the Avogadro number; z_i is the number of valence electrons, $z_F = 1$; ρ_i^{m} is the density of element dissolving in metallic state, for fluorine the density is taken in solid state $\rho_F = 1.3$ g/cm^3; A_i is the relative atomic mass.

It was obtained as a result calculation that the initial heat of fluorine dissolution in molten iron is 314766 J/mol. Using the statements of theory of quasi-regular solutions, we shall obtain the isobar-isothermal potential of expression (15) with numerical values:

$$\Delta G_{12} = 314766 - 45\,T. \qquad (21)$$

Then, the expression of this potential for reaction (11) will have a form:

$$\Delta G_9 = \Delta G_5 - \Delta G_{10} - 2\Delta G_{12} = -1762732 + 233\,T. \ (22)$$

From expression of constant of equilibrium reaction (11)

$$K_9 = \frac{a_{(CaF_2)}}{a_{[Ca]}\, a_{[F]}^2} \qquad (23)$$

at the assumption that temperature at slag−metal interface is 1873 K, the activity of calcium in melt is equal to its solubility in a pure molten iron, i.e. 0.0001 wt.% [33], and the activity of calcium fluoride in slag is equal to 1, we shall find the partial pressure of fluorine at slag−metal interface $P_{F_2}^{II} = 5.6 \cdot 10^{-11}$ Pa.

Comparing the partial pressure of fluorine at different slag phase interfaces, we state the presence of gradient of fluorine concentrations directed to metal that leads to the appearance of fluorine flow directed from the metal. The fluorine flow in its turn causes the formation of the nitrogen flow directed opposite to it.

Thus, it is possible to realize the alloying of metal remelted with nitrogen from a gas phase in ESR in a chamber furnace in nitrogen atmosphere using slags of Ca−CaF$_2$ system at the expense of «pumping» effect.

1. Lakomsky, V.I. (1974) *Plasma-arc remelting*. Kyiv: Tekhnika.
2. Grigorenko, G.M., Pomarin, Yu.M. (1989) *Hydrogen and nitrogen in metals during plasma melting*. Kyiv: Naukova Dumka.
3. Rashev, Ts. (1981) *Production of alloy steel*. Moscow: Metallurgiya.
4. Paton, B.E., Medovar, B.I., Saenko, V.Ya. et al. (1990) Position of electroslag technology in production of high-nitrogen steels. *Problemy Spets. Elektrometallurgii*, **3**, 4−13.
5. Paton, B.E., Medovar, B.I., Lebedev, V.K. et al. (1990) Nitriding of liquid metal from gas phase in pressure slag arc remelting. *Ibid.*, 14−18.
6. Svyazhin, A.G. (1990) Nitrogen alloying of steel. *Chyorn. Metallurgiya, Bull. NTI*, **6**.
7. Paton, B.E., Medovar, B.I., Grigorenko, G.M. et al. (1991) Nitriding processes in slag arc remelting. *Problemy Spets. Elektrometallurgii*, **3**, 14−16.
8. Takaki, S., Tsuchiyama, S., Ito, H. et al. (2000) Microstructure and mechanical properties of high nitrogen austenitic steels produced by nitrogen absorption at solid state. *Current Advances in Materials and Processes*, **3**, 364−365.
9. Kataoka, K., Tsuchiyama, S., Takaki, S. (2000) Microstructure and mechanical properties of high nitrogen austenitic steels produced through mechanical milling process. *Ibid.*, 358−361.
10. Gotin, V.N., Shalimov, Al.G. (1993) Vacuum arc remelting of steels and alloys with specified content of nitrogen. *Stal*, **11**, 32−35.
11. Kats, Ya.L., Laktionov, A.V., Okorokov, G.N. (1990) Interaction between nitrogen and metallic melts during va-cuum-plasma heating. Part 1. *Problemy Spets. Elektrometallurgii*, **3**, 82−87.
12. Kats, Ya.L., Laktionov, A.V., Okorokov, G.N. (1990) Interaction between nitrogen and metal melts during vacuum-plasma heating. Part 2. *Ibid.*, **4**, 88−91, 107.
13. Lejbenzon, V.A., Kazakov, S.S., Sadovnikov, Yu.V. et al. (1999) Melting of high-nitrogen Cr−Ni−Mn steels by gas-oxygen refining method. *Stal*, **8**, 18−20.
14. Paton, B.E., Lakomsky, V.I., Torkhov, G.F. et al. (1975) Production of high-nitrogen steels and their properties. *Problemy Spets. Elektrometallurgii*, **1**, 68−88.
15. Imamutdinov, I. (2002) More nitrogen steel for the country. *Ekspert*, **5**, 24.
16. Morozov, A.N., Ponomarenko, A.G., Kozlov, Yu.E. (1971) On solubility of nitrogen in slags. *Izv. AN SSSR, Metally*, **6**, 53−57.
17. Ponomarenko, A.G., Kozlov, Yu.E., Morozov, A.N. (1974) On solubility of nitrogen in slags. *Ibid.*, **3**, 64−68.
18. Utochkin, Yu.I., Pavlov, A.V., Frojde, T. et al. (1993) Influence of oxidizing potential on solubility of nitrogen in slag melts. *Izv. Vuzov, Chyorn. Metallurgiya*, **3**, 10−15.
19. Grigoryan, V.A., Belyanchikov, L.N., Stomakhin, A.Ya. (1987) *Theoretical principles of electric steel-making processes*. Moscow: Metallurgiya.
20. Yavojsky, V.I. (1952) *Gases in metal pools of steel-making furnaces*. Moscow-Sverdlovsk: Metallurgizdat.
21. Morozov, A.N. (1968) *Hydrogen and nitrogen in steel*. Moscow: Metallurgiya.
22. Stomakhin, A.Ya. (1970) On interaction between metal melt and nitrogen in electric arc. *Izv. Vuzov, Chyorn. Metallurgiya*, **4**, 87−90.
23. Morozov, S.S., Kryakovsky, Yu.V., Safronov, A.A. et al. (1987) Behaviour of nitrogen during melting of high-quality steels in different steel-making units. *Ibid.*, **5**, 28−32.
24. Ryabtsev, A.D., Troyansky, A.A. (2001) Production of ingots from titanium, chrome and alloys on their base in chamber furnaces with use of «active» metal-containing fluxes. *Problemy Spets. Elektrometallurgii*, **4**, 6−10.
25. Linchevsky, B.V. (1986) *Thermodynamics and kinetics of interaction between gases and liquid metals*. Moscow: Metallurgiya.
26. Ryabtsev, A.D. (1999) Unit for electroslag remelting of high-reactive metals and alloys with use of active calcium-containing fluxes in controllable atmosphere or vacuum. In: *Transact. of DonGTU on Metallurgy*, Issue 14. Donetsk.
27. Troyansky, A.A., Yaroshenko, A.P., Savoskin, M.V. et al. (1999) Application of thermally split graphite as a thermal- and gas-insulating coating during electroslag remelting of steels and alloys. *Problemy Spets. Elektrometallurgii*, **3**, 9−15.
28. Mogutnov, B.M., Tomilin, I.A., Shvartsman, L.A. (1984) *Thermodynamics of iron alloys*. Moscow: Metallurgiya.
29. Grigoryan, V.A., Stomakhin, A.Ya., Ponomarenko, A.G. et al. (1989) *Physical-chemical calculations of electric steel-making processes*. Moscow: Metallurgiya.
30. (1997) *Properties of elements*. Handbook. Vol. 2. Ed. by M.E. Drits. Moscow: Metallurgiya.
31. Rudnitsky, L.A. (1979) Some surface and volume properties of solids in terms of electronegativity. *Zhurnal Fiz. Khimii*, **12**, 3003−3010.
32. Ashkroft, N., Mermin, N. (1979) *Physics of solids*. Moscow: Mir.
33. Kubashevsky, O. (1985) *Constitution diagrams of binary systems on iron base*. Moscow: Metallurgiya.

APPLICATION OF MAGNETODYNAMIC UNIT IN THE TECHNOLOGY OF ELECTROSLAG CLADDING OF STEEL MILL ROLLS USING A LIQUID METAL

V.I. DUBODELOV, V.K. POGORSKY, V.K. SHNURKO, P.I. ZAGOROVSKY, V.B. SHABANOV,
O.V. SVIRIDOV, V.E. PANCHENKO and V.G. GAPONOV,
Physical-Technological Institute of Metals and Alloys, NASU, Kyiv, Ukraine

Different types of equipment for steel casting are considered. The use of a magnetodynamic unit for overheating and pouring of iron-carbon alloys as a link in the technological diagram of the electroslag cladding of mill rolls is offered.

K e y   w o r d s: *magnetodynamic unit, electroslag cladding, liquid (molten) metal, mill roll, steel, metal heating, casting (pouring)*

The electroslag cladding of steel parts using a liquid metal belongs to one of the most effective technologies in special electrometallurgy [1]. Realization of this method in industry requires the use of units for a controllable feeding of liquid filler metal into a mould. Analysis of the process of electroslag cladding of steel parts shows that the pouring unit should satisfy the following requirements: useful capacity of not less than the mass of one layer of cladding; feasibility of long-time holding and, when necessary, melt preheating up to 1550–1600 °C; provision of continuous or periodic portion feeding of melt into a mould with a preset consumption.

In steel-making industry the molten steel is poured mainly by ladles with use of bottom-tap devices or a gate to control the melt consumption or to cut off the jet. This equipment for the technology with a long-time cycle of steel pouring with small portions (1–10 kg) and consumption (0.1–5.0 kg) is not suitable, because it is difficult to realize these conditions using above-mentioned executive mechanisms.

Electric technological units, including those of magnetodynamic type, which are widely used in foundry in manufacture of castings from non-ferrous alloys and cast iron, meet most completely the above-mentioned requirements [2].

The known magnetodynamic units used for preheating and pouring of molten cast iron can serve a basis for the creation of similar equipment for steel pouring. In some case, in pouring of high-carbon alloyed grades of steels with 1450–1500 °C liquidus temperature in particular, they can be used without significant changes in design.

In optimizing the process of electroslag cladding of steel mill rolls of 700–800 mm diameter the tech-nological diagram envisaged the use of an electric furnace, magnetodynamic unit for holding and pre-heating of melt and intermediate chute for feeding the liquid metal into the mould[*] (Figure).

For practical realization of rolls cladding with account for requirements of the technology, chemical composition of filler melt and temperature of its pouring, the magnetodynamic unit of the MDN-6ch-3.0-2 type was used.

The selection of this unit was stipulated by the fact that useful capacity of the unit crucible guaranteed the necessary stock of liquid metal, the inductor power allowed its heating and long-time holding at 1500–1550 °C temperature, and the electromagnetic system provided the metal consumption in pouring up to 5–7 kg/s. In addition, this unit could, when necessary, correct chemical composition of the melt by adding ferroalloy and charge materials. The unit of the above-mentioned modification was equipped with an induction part which included an inductor, electromagnet, refractory block with a E-shaped channel and two pouring lips.
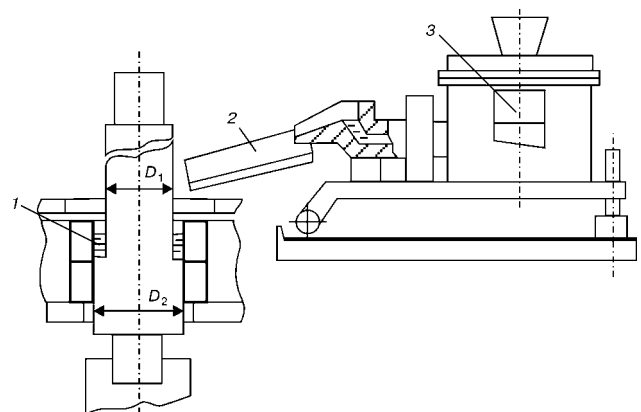
Layout of equipment in electroslag cladding of mill rolls: *1* — electroslag furnace; *2* — chute for melt feeding to the mould; *3* — magnetodynamic unit

---

[*]Idea of use of the magnetodynamic unit in the technological process of electroslag cladding with liquid metal of mill rolls belongs to Prof. Boris I. Medovar.

The experience of application of magnetodynamic units for pouring of low-carbon steel showed that their serviceability depends mainly on the life of refractory lining [3]. Therefore, a special attention was paid during experiments to the problems of technology of manufacture, resistance and service life of the lining in parallel with study of peculiarities of operation of electromagnetic systems of the equipment used for mill roll cladding.

In testing technology of electroslag cladding of steel mill rolls with a working layer from high-speed steel [4] the lining of the crucible working layer and unit channel was manufactured from mullite-corundum mass with a high content of aluminium oxide. Before putting this unit into operation the lining was heated up to 900−1000 °C with gas torches, mounted in the crucible. Heating of the channel lining was made by injection of overheated air from the crucible working space into the channel cavity. To decrease the heat load, to prevent thermal shock on not yet sintered working layer of lining, the unit was put into operation using Fe−C melt with a high content of carbon and silicon.

The initial metal was melted in arc furnace. At the 1550 °C melt temperature in furnace, it was poured into a bottom-tap ladle and fed to the magnetodynamic unit. 2000 kg of melt was poured into the unit crucible, its temperature in this case was reduced by 100−150 °C. Inductors for metal preheating were switched on. After 20−30 min the metal temperature in the unit was stabilized and then increased as a result of its induction heating in channels and heat transfer to the crucible due to magnetohydrodynamic and convective flows in the channel−crucible system of the unit.

After sintering of the lining working layer the peculiarities of operation of the magnetodynamic unit using molten steel, in particular characteristics of electromagnetic systems, conditions of heating and stabilization of melt temperature, effect of technological parameters on accuracy of proportioning and chemical composition stability were determined.

Nature of change of metal temperature in the unit depending on the supplied power was studied. It was established that, by changing the total power of inductors within the 110−230 kW ranges, it is possible to control the melt temperature in the conditions of holding and pouring, and also during adding of alloying elements to the melt for correction of its chemical composition.

In cladding of a pilot batch of mill rolls the initial melt was produced in arc furnace and the alloying elements were added for making steel of a chemical composition required by the technology. At 1600−1620 °C temperature in the furnace the molten steel was poured into a bottom-tap ladle and then poured into a magnetodynamic unit, from which the sampling was made for the melt chemical analysis. When necessary, the ferroalloys were added to the unit crucible to correct the steel chemical composition. The main

technological parameters, which should be provided by the unit in roll cladding, are the stability of chemical composition, temperature of pouring and mass of poured portion of filler melt for increment.

In steel pouring into the mould the constant electrical parameters were mainly maintained in electromagnetic systems of the unit. After melt pouring from the unit its mass was decreased. This led to some increase in metal temperature. If necessary, the temperature of the melt was corrected by changing supply voltage of the induction part by 30−40 V.

Before the roll cladding the melt portions, poured by each lip of the unit, were calibrated, and such supply voltages of electromagnetic systems were set which provided the minimum deviation of mass portion from the preset value.

According to the technology developed for steel mill roll cladding, the steel melt was fed to the mould by portions using a magnetodynamic unit with a cycle of a portion pouring by a preset program. Command for portion pouring was given by an operator from the control panel equipped with a computer system of diagnostics of technological parameters of the roll cladding process. The value of portion was corrected by an operator, changing the time of proportioning. The melt was fed to the mould in an intermediate chute. At its cleaning from scrap, a spare chute was used. Here, the voltage was supplied to an additional electromagnet. 2.0−2.2 t of wear-resistant material were deposited on the steel roll surface during 3.0−3.5 h. In non-working shifts the unit was operated in the condition of steel holding. In this case, the voltage for induction part of the unit was reduced and melt temperature in the range of 1450−1480 °C was kept.

The complex of works made it possible to define the rational technological parameters of the process of pouring high-speed steels and confirmed the serviceability of the used magnetodynamic unit. This gave an opportunity to create an effective domestic complex of electroslag cladding of working mill rolls of 700−800 mm diameter and 2000−2500 mm length of working part and to organize the serial producing of rolls whose wear resistance 4−4.5 times increases the wear resistance of rolls manufactured by the traditional technology [4, 5].

1. Medovar, B.I., Medovar, L.B., Tsykulenko, A.K. et al. (1999) On problem of electroslag melting of large-tonnage billets from high-alloy special steels and alloys. *Problemy Spets. Elektrometallurgii*, **2**, 26−30.
2. Polishchuk, V.P., Tsin, M.R., Gorn, R.K. et al. (1989) *Magnetodynamic pumps for liquid metals*. Kyiv: Naukova Dumka.
3. Polishchuk, V.P., Pogorsky, V.K., Gorn, R.K. (1987) Test of hydrodynamic pouring device for steel in industrial conditions. In: *Abstr. of pap. of 12th Meeting on Magnetic Hydrodynamics in Riga*. Salaspils: Institute of Physics of AN Latv. SSR. Part 4.
4. Shabanov, V.B., Sviridov, O.V., Belobrov, Yu.N. et al. (1999) Creation of electroslag cladding complex with liquid filler metal of hot mill working roll for continuous wide-strip mills. *Avtomatich. Svarka*, **3**, 51−54.
5. Medovar, L.B., Chernets, A.V., Grabovsky, Ts.F. et al. (2000) Experience of manufacture and application of high-speed steel rolls using ESC with of liquid metal. *Problemy Spets. Elektrometallurgii*, **3**, 3−9.

APPLICATION OF ELECTROSLAG PROCESS WITH NON-CONSUMABLE ELECTRODES FOR MELTING, REFINING AND TREATMENT OF METALS.
Part 1

F.K. BIKTAGIROV

The E.O. Paton Electric Welding Institute, NASU, Kyiv, Ukraine

Technologies of electroslag treatment of metals in which the electroslag process is realized using non-consumable electrodes are considered. The capabilities of electroslag heating and refining of molten metals to improve the metal production quality are shown.

Key words: *electroslag process, non-consumable electrode, electroslag casting, refining, heating, metal quality*

Electroslag remelting and other varieties of melting in a slag melt of the consumable electrode have found a wide spreading as effective processes of improving quality of metal products which is attained also owing to metal refining with a slag. In these technologies the slag is heated by a heat generated in it during passing the current supplied by one or several metal electrodes which are current-carrying elements and objects of melting simultaneously. At the same time, because of various reasons, there appears often a need in slag heating without the use of the consumable electrode. These reasons may be, for example, impossibility, complexity or expensiveness in manufacture of the consumable electrode; absence of need in additional enter of molten metal from the consumable electrode; impossibility of fulfillment of requirements for the composition and temperature of slag in use of the consumable electrode. Therefore, the technologies based on conductance of the electroslag process using non-consumable electrodes were developed at the E.O. Paton Electric Welding Institute in parallel with a classical electroslag remelting. Typical graphitized electrodes are used more often as the latter, but, when necessary, the metal water-cooled electrodes with a working part of different current-conducting materials, including refractory metals, immersed into a slag melt, are used.

Electroslag technologies with non-consumable electrodes used for melting, refining and casting of metals can be divided conditionally into two large groups. The first group includes technologies where the molten metal, preliminary prepared in any melting unit, is subjected to electroslag treatment. The second group includes technologies where the initial metal is in a solid state and its treatment is accompanied by a partial or complete melting. Technologies related to the production of ingots from steels and alloys are most typical of the first group. This is electroslag

heating of a head part of ingots, electroslag casting and portion electroslag casting.

The aim of the electroslag heating is to decrease the shrinkage cavity and to reduce the top discard. The technology of electroslag heating was successfully implemented by the associates of the PWI at several metallurgical and machine-building plants as far back as at the end of the 1950s and beginning of the 1960s of the last century [1, 2]. Technological scheme of electroslag heating is presented in Figure 1. A special water-cooled or lined hot top is mounted on a cast iron mould. After filling this hot top with a molten metal the slag is melted using non-consumable electrodes. During ingot formation its head part is heated with an overheated slag and the metal is maintained in this region in a molten state.

The electroslag heating improves the structure of the head part of the ingot and prevents the appearance of coarse defects of a shrinkage origin, thus providing the decrease in a top discard and increase in the efficient metal output. At the same time the electroslag heating does not influence in principle on the formation of other defects typical of ingots of the traditional methods of production. It can be only noted that the refining of metal volumes adjacent to the slag is occurred in this case and some decrease in the zone of a negative liquation in the ingot bottom part is observed.

To increase the quality of the metal products more significantly a method of electroslag casting (ESC) has been developed [3, 4]. The principle of this method is as follows. A slag pool is set and heated to the required temperature in a water-cooled mould using non-consumable electrodes (Figure 2). Then, a molten metal is poured through a slag into the mould, which is solidified during the electroslag heating under the condition of removing the shrinkage cavity with a gradual decrease in power supplied to the slag pool. After heating completion and complete solidification
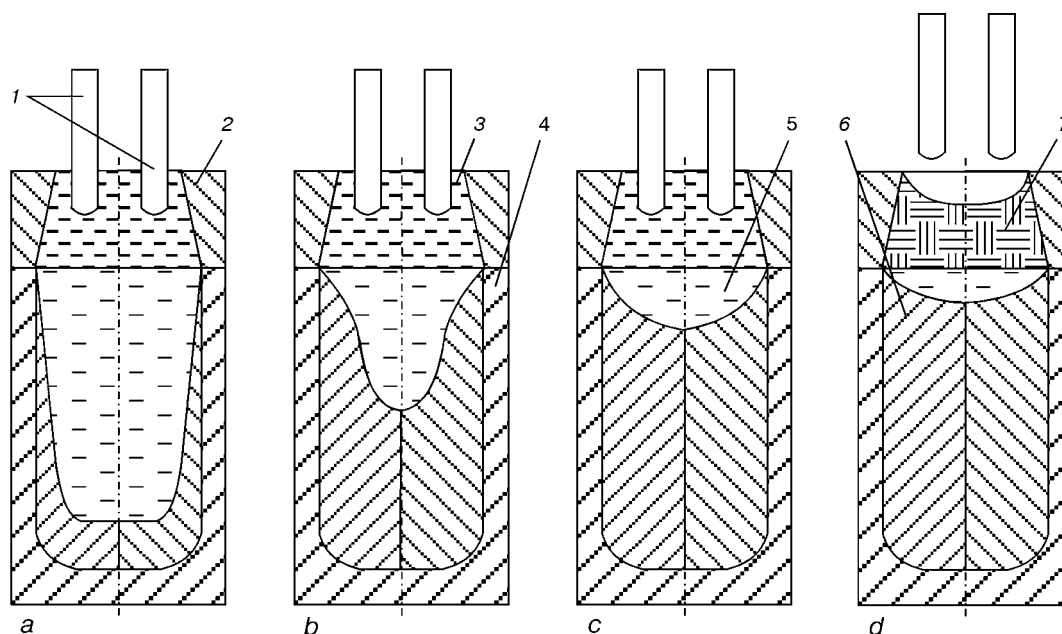
Figure 1. Scheme of electroslag heating of a head part of ingot: *1* — electrodes; *2* — hot top; *3* — molten slag; *4* — mould; *5* — molten metal; *6* — solid metal; *7* — solid slag

of the slag and metal the ingot produced is withdrawn from the mould.

Using this general technological diagram, the real realization of this method can be different. For example, all the described method can be performed in a water-cooled mould mounted on a flat water-cooled bottom plate. Or, a conventional cast iron mould can be mounted on a water-cooled bottom plate including all the volume of a slag melt, and different types of hot tops are mounted on this mould. The casting can be performed both into a movable mould, when the level of the metal poured is kept constant and to a

fixed mould. In the latter case the current-carrying electrodes are gradually moved upward during the mould filling. Slag can be melted from initial solid components directly in a mould or in a separate flux-melting furnace and poured to the mould before the metal casting. Electrical diagram of the electroslag heating can be single- or three-phase with different methods of electrodes connection to the power source.

In spite of many variants of the ESC methods, they have common features defining the quality of the ingots produced. Firstly, the metal is treated intensively with a slag, entrapped into the thickness of
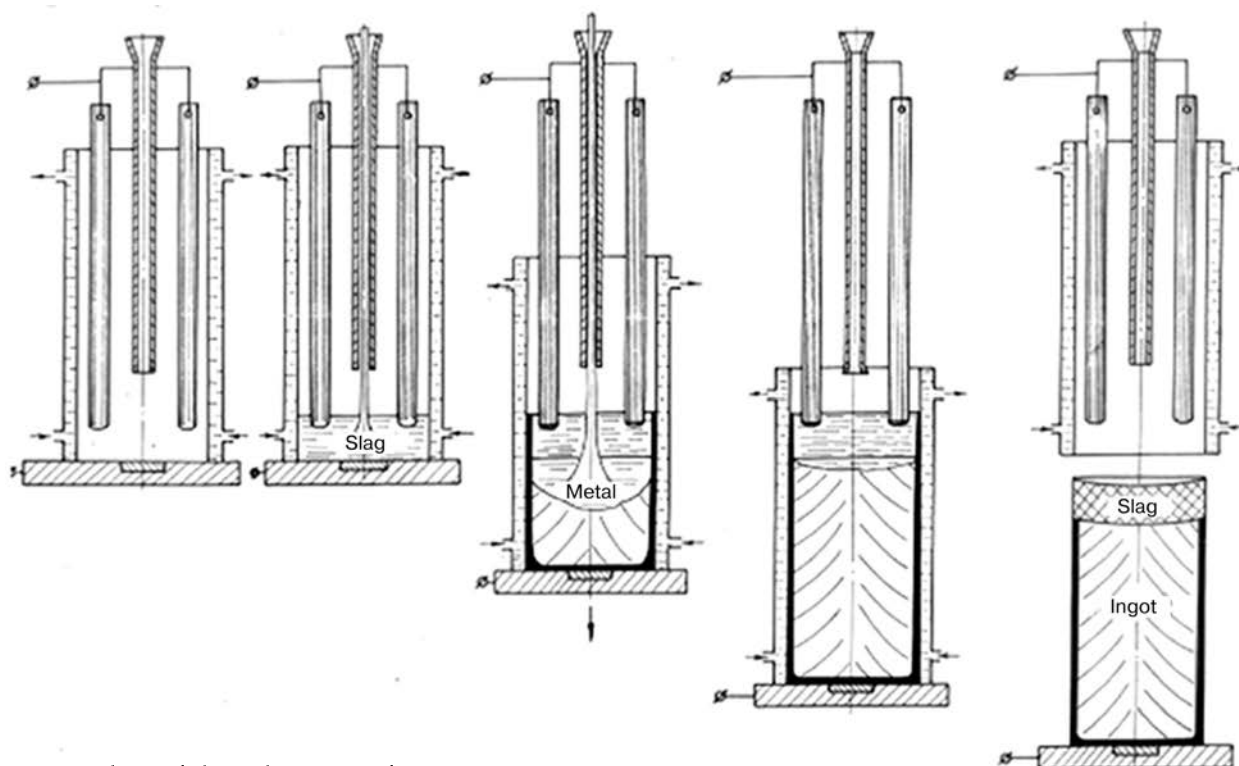

Figure 2. Scheme of electroslag casting of ingots

metal melt being poured by a stream. Calculations and model experiments showed that during this period from 2 to 5 % of all the amount of slag is available in the metal pool, and the reaction surface of the interacting phases is increased of tens and hundreds times. Secondly, during electroslag casting the slag protects metal from a direct contact with the surrounding atmosphere that reduces its oxidation and probability of formation of secondary non-metallic inclusions. In addition, inclusions of endogeneous and exogeneous origin are assimilated with a slag both in casting and during all the period of the ingot formation. Thirdly, in metal casting under slag a thin slag layer, a skull, is formed between the ingot lateral surface and mould, that promotes the formation of a defect-free surface of the ingot.

The above peculiarities of the electroslag casting provide a complex improvement of the quality of ingots produced. Numerous investigations of ESC ingots of mass from 2 to 75 tons, produced from roll, stamp, rotor, ball-bearing and stainless steels, and also heat-resistant alloys confirm this. At a properly selected technology there is no closed shrinkage cavity in the ESC ingots. In the head part only a negligible cup-like depression is available whose sizes in axis do not exceed 3–5 % of the total ingot length. The bottom part of ingots is dense and homogeneous due to cooling action of the bottom plate, therefore, there is no need in a bottom discard. However, the head part of ESC ingots is either not removed or removed very little. The surface of the ingots produced is smooth, without cracks, corrugations, films and solidified metal spatters, that almost excludes the need in its trimming or cleaning before subsequent processing. Distribution of elements in height and section of these ingots is more uniform, and a zonal and different types of a local chemical inhomogeneity, in particular V- and Λ-shaped liquation, are expressed not so clearly as in similar ingots of the conventional production. Content of sulphur and non-metallic inclusions in metal of ESC ingots is 1.5–2 times lower than in a ladle sample [5].

The improvement of quality of ESC ingots has a positive effect on service properties of products manufactured from them. Thus, mechanical properties, in particular characteristics of ductility and impact strength of structural and stainless steels are increased by 15–25 %, and the service life of dies and cold mill rolls is increased by 20–40 %. The ESC method is especially effective in production of ingots from complexly-alloyed steels and alloys, as the extra expenses are well compensated by metal saving due to increase in efficient metal output and elimination of the surface cleaning.

ESC provides good conditions of formation of a crust zone and metal refining from non-metallic inclusions and harmful impurities, improves the structure of head and bottom parts of the ingot. However, it does not make it possible to influence actively on conditions of solidification of the ingot central regions. The appearance of several defects of structure of steel ingots is associated often with those processes proceeding in these mentioned zone, in particular with the formation of an extended two-phase zone. In solidification of metal, poured into the mould, the boundary of beginning its solidification (liquidus line) after removing of inner heat of overheating, is moving quickly upwards that causes the formation of a wide region of a solid-liquid state. In ESC the limiting effect of heating on movement of the solidification front is valid only for the depth of $1/3-1/2$ of the ingot diameter, therefore, the underlaying volumes of metals are solidified almost at the same conditions as in the conventional ingot.

It is known that one of the main means of improving the physical and chemical homogeneity of the ingot is the organizing of successive solidification of metal in a vertical direction using a shallow metal pool and high temperature gradient in it. To attain these conditions a method of a portion electroslag casting (PESC) has been developed at the PWI [6, 7].

It differs from the ESC by that the metal is poured into the mould not at once, but in several procedures. Firstly, the first portion is poured through a molten slag, which fills only a part of the mould volume (Figure 3). After this pouring the metal mirror is subjected to electroslag heating using conditions which keep the portion upper part molten. Here, the poured metal is solidified gradually upwards. After a definite time, when a small amount of molten metal is remained under the slag layer, the second portion of metal is poured to the mould which is also subjected to holding at the electroslag heating and solidified in an axial direction. The similar pouring of metal with small portions is repeated until the full filling of the mould. At the final stage of formation of PESC ingot the power supplied to the slag pool is decreased gradually to remove the shrinkage cavity.

Using this method of ingot casting there is a feasibility to provide upward successive metal solidifying with a presence of a comparatively small metal pool at each moment of time. With a change in such PESC parameters, as volume and height of portions, time of holding, temperature of slag pool can govern the process of solidification and create the favourable conditions of the ingot formation.

The PESC method has passed a comprehensive experimental-industrial testing in production of ingots of mass from 5 to 200 t and of different steel grades. Under optimum conditions of the electroslag heating, especially in the period before the pouring of next portion, the ingots produced had a good surface, at which the interface between the portions was distinguished in the form of not deep smooth narrowing of up to 2–3 mm. They did not make obstacles for the further processing of ingots and did not require any preliminary machining.

Examination of macrostructure and sulphur prints of longitudinal axial templets showed that there is no V-shaped liquation and other axial defects in the
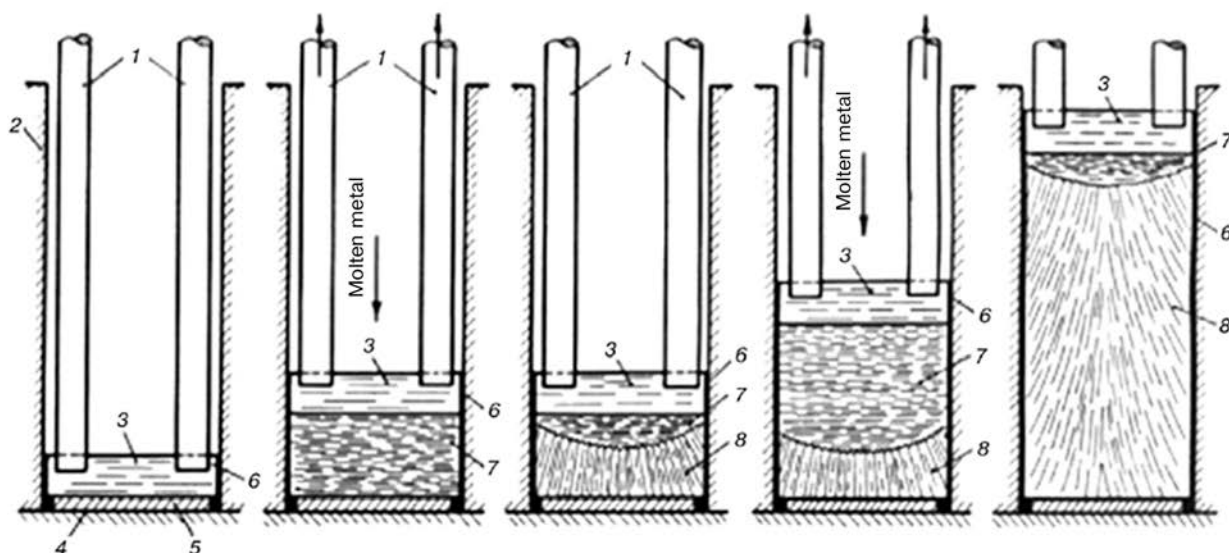
Figure 3. Scheme of a portion electroslag casting: *1* — non-consumable electrodes; *2* — mould; *3* — slag pool; *4* — bottom plate; *5* — primer; *6* — skull; *7* — metal pool; *8* — solid metal

form of porosity, clusters of segregates and inclusions in the PESC ingots produced even from steels having a wide interval of solidification (such as ShKh15, 9Kh and 9KhM) unlike the traditional ingots. An off-axis Λ-shaped liquation is either absent or expressed slightly, which is shown in the sulphur prints in the form of separate short lines. The shrinkage cavity in the head part is absent, and the density of the cast metal of the PESC ingots is much higher

than that in ingots of a conventional casting. It this case it is not decreased abruptly from the surface to the center, but it has often the tendency to the increase in this direction (Figure 4). The metal refining with a slag under the PESC conditions is more effective than that in ESC. This is explained by smaller volumes of metal poured through the slag and longer metal holding under the slag. The content of sulphur and sulphide inclusions is reduced usually by 2−3 times and oxide inclusions — by 1.5−2 times, and their distribution in height and section of the PESC ingot is comparatively uniform.

Taking into account that the PESC ingot consists as if of separate molten-state fused parts, a special attention was paid to the examination of quality of the transition zone between the portions. It was revealed that the ingot macrocrystalline structure can be different depending on the physical-chemical properties of the casting metal. In one case a narrow zone of fine-grained crystals is formed by the contour of a metal pool which existed by the moment of pouring the next portion, and then the column crystals are followed. In another case the structure of ingots is approximately the same, but the fine crystals are not formed at the interface between the portions. In the third case the crystals change only their orientation.

However, during examination of the microstructure the zone of fusion was not revealed. This zone was not also revealed on the macrotemplets after treatment of ingots by pressure (forging, rolling) and heat treatment. It was established that the visible conditional interface between portions during macroetching of the initial metal is not a defect of the PESC ingot structure, but it reflects only the change in heat conditions of formation of the primary crystalline structure. Moreover, the examination of the chemical composition, density and mechanical properties showed that the metal in the transition zone possesses the better characteristics than those beyond it.
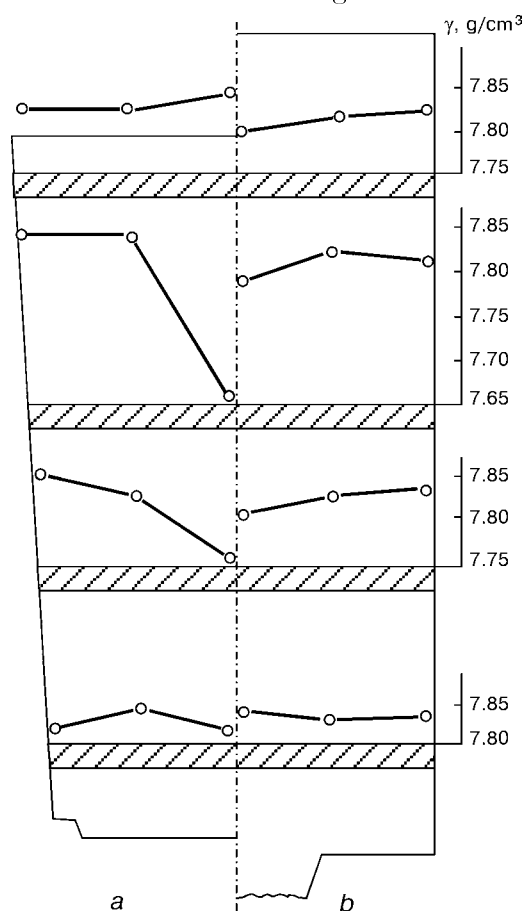

Figure 4. Density of cast metal of a conventional (*a*) and PESC (*b*) ingot

High quality of the PESC ingots is attained owing to the favourable conditions of metal transition from liquid to solid state. Figure 5 presents, as an example, the results of a mathematical modelling of change in depth of metal pool, H_p, and extension of two-phase zone in an axial zone, B, of 75-ton PESC 1800 mm diameter ingot produced from rotor steel. At total length of more than 3500 mm the pool depth on liquidus line does not exceed 1300 mm, and maximum size of two-phase zone is only about 150 mm. For comparison, according to data of [8] the coarse liquation defects are observed in that case in ESR of 50-ton ingot produced from the similar class of metal, when the distance between the isotherms of liquidus and solidus exceeds 200—300 mm. The examination of dispersity of structure of the mentioned PESC ingot showed that the distance between the secondary axes of dendrites, and this parameter being closely associated with sizes of the two-phase zone, is varied from 0.18—0.25 near the surface up to 0.35—0.45 mm in axial zones. In addition, the density of a dendritic structure is increased in the zones of coalescence of portions. The similar data of crystalline structure of ingots of conventional production are much worse, that is proved by comparison of characteristics of a dendritic liquation, reflecting the conditions of formation of a primary structure (Figure 6). As is seen, the PESC metal is close by this parameter to the ESR metal and greatly superior to the conventional metal.

Purity, density and homogeneity of the PESC metal contribute, naturally, to the mechanical properties of products, manufactured from them, whose level exceeds usually the requirements of technical specifications. Moreover, the combination of high strength and ductility is characteristic here, which is very important sometimes for a number of domestic critical products, such as cold mill rolls or turbine rotors. The high quality of the PESC metal allows sometimes its use even without a pressure treatment. For example, the service life of dies (steel of 5 KhNM grade) manufactured of PESC ingot of 5 t mass is not inferior to the serviceability of dies manufactured from a forged metal of a conventional production.

The portion electroslag casting is used mainly for production of large forge ingots as a means of prevention of defects of liquation and shrinkage origin, whose formation in a conventional casting is increased with increase in the ingot mass. However, this casting is not less effective also in producing comparatively small ingots of mass of several tons, in particular from metals susceptible to liquation and formation of a coarse cast structure during the process of solidification. Metal pouring by portions and their fusion in a molten state can also be a way of enlargement, making it possible to produce billet of a much larger mass, as was shown on the example of producing ESC ingots of nickel, using a melting unit of a comparatively low capacity [9, 10].

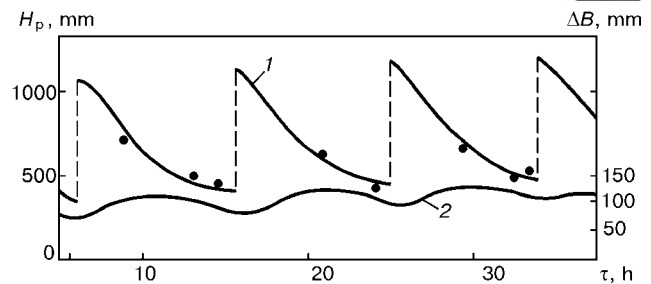Except the above-described methods of casting of ingots, the electroslag process with non-consumable

Figure 5. Change in depth of metal pool (*1*) and width of two-phase zone (*2*) in process of PESC of 75-ton ingot from rotor steel

electrodes is also used successfully for other types of treatment of molten metal, for example, for refining and overheating of copper, copper and aluminium alloys, cast iron [11]. In this case a slag pool is set in a special lined vessel, then a molten metal, melted in induction furnace or other melting unit, is poured into this vessel. During pouring an intensive stirring of slag and metal and refining of the latter are occurred. Further, the metal melt is subjected to holding under the slag heated by non-consumable electrodes, that makes it possible to realize a controllable metal heating and its additional treatment, including ingredients specially added to slag or metal. The molten metal prepared is periodically or continuously poured from the melting vessel.

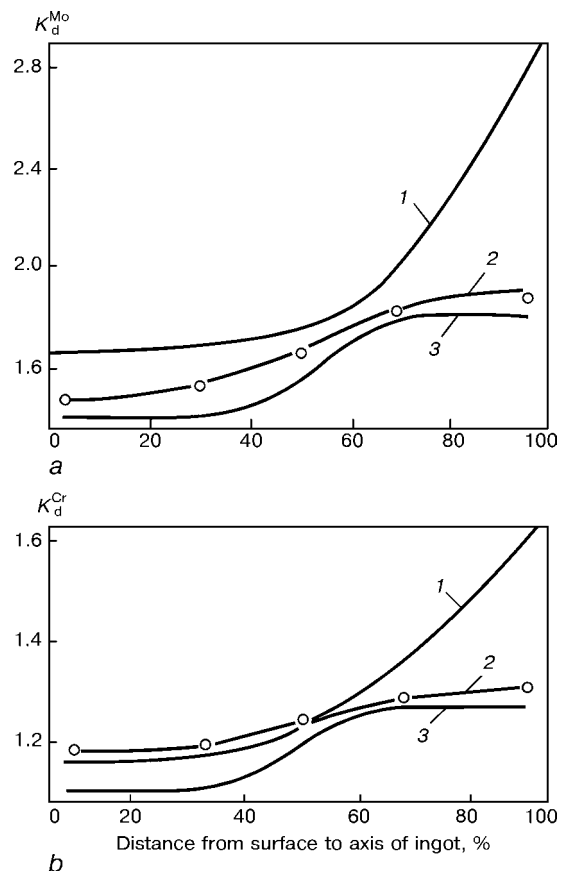According to data of [11], in electroslag treatment of molten copper the concentration of oxygen is re-

Figure 6. Change in coefficient of dendritic liquation, K_d, of molybdenum (*a*) and chromium (*b*) in section of rotor steel ingot of 75—100 t mass: *1* — conventional ingot; *2* — PESC ingot; *3* — ESR ingot

duced by one order, sulphur and non-metallic inclusions are reduced by several times in it. In similar treatment of aluminium alloys the gas saturation and contamination of metal are decreased. For example, in alloy Al−6.2Mg the contamination with oxide films was reduced from 0.294 to 0.003 mm^2/cm^2 [12]. It is considered that the electroslag refining is most effective among the known methods of purification of aluminium alloys. In electroslag treatment of cast iron the effect of modifying metal with Mg- and Ca-containing components of slag is attained, except decrease in concentration of gases, non-metallic inclusions and sulphur [13]. It is expressed in refining of precipitations of graphite and changing its shape from plate- to more favourable vermicular-type. Due to this, when necessary to produce graphite of a nodular shape in cast iron the consumption of modifiers (cerium, magnesium, REM and others) can be decreased approximately twice. As a result, the metal modifying, increase in its purity and temperature promote increase in strength and ductile properties of cast iron and quality of products produced.

Method of electroslag heating of steel in an intermediate ladle (tundish) in continuous pouring is very similar by the design and technological procedures to the methods of electroslag treatment of non-ferrous metals and cast iron [14]. The aim of this heating is the compensation of heat losses from the intermediate ladle and keeping the metal temperature in narrow ranges during long time. This is very important from the point of view of stabilization of the process of pouring, especially at metal temperatures close to the liquidus temperature. In use of the slags of CaF_2−CaO−Al_2O_3–SiO_2 system, typical of electroslag process, the metal heating occurs simultaneously with its refining from sulphur. From the data of authors of the present work the concentration of sulphur is decreased from initial 0.015−0.025 to 0.005−0.010 %. In addition, these slags assimilate non-metallic inclusions, in particular aluminium oxides, that reduces greatly the hazard of sticking of pouring sleeve lip with metal.

The above-described examples of electroslag treatment of molten metals prove wide opportunities in use of similar technologies for improving quality of metal products. The application of electroslag process with non-consumable electrodes is not less effective for melting and refining of solid metals. This information will be given in Report 2 of this article.

1. Tyagun-Belous, G.S., Dudko, D.A. (1958) Electroslag heating with non-consumable electrodes of ingot heads and shaped castings. *Avtomatich. Svarka*, **10**, 36−43.
2. Bakumenko, S.P., Gulyaev, B.B., Verkhovtsev, E.V. (1967) *Decrease of steel ingot waste*. Moscow: Metallurgiya.
3. Latash, Yu.V., Pshenichny, B.A., Voronin, A.E. et al. (1984) Electroslag casting of ingots from high-alloy steels and alloys. *Stal*, **9**, 35−37.
4. Bastrakov, N.F., Tulin, N.A., Nemchenko, V.P. et al. (1978) *Electroslag pouring of steel*. Moscow: Metallurgiya.
5. Biktagirov, F.K., Latash, Yu.V., Pshenichny, B.A. et al. (1997) Electroslag casting of ingots in UO-106 unit. *Problemy Spets. Elektrometallurgii*, **2**, 7−11.
6. Latash, Yu.V., Voronin, A.E., Nikolaev, V.A. et al. (1975) New process of production of high-quality large forging ingots. In: *Problems of special electrometallurgy*, Issue 2.
7. Latash, Yu.V., Voronin, A.E., Nikolaev, V.A. (1975) Production of high-quality large ingots by portion electroslag casting. *Stal*, **11**, 999−1002.
8. Niimi, T., Miura, M., Matsumoto, S. et al. (1975) Evaluation of large ESR ingot. In: *Electroslag remelting*. Kyiv: Naukova Dumka.
9. Tynyankin, V.B., Latash, Yu.V., Krutikov, R.G. et al. (1990) Producing of nickel slabs by portion electroslag casting method. *Problemy Spets. Elektrometallurgii*, **3**, 24−29.
10. Latash, Yu.V., Krutikov, R.G., Tynyankin, V.B. et al. (1990) Portion electroslag casting of NP-2 nickel ingots. In: *Transact. on Advanced Processes of Melting and Casting of Non-Ferrous Metals*. Moscow: TsNIITMASh.
11. Lyuty, I.Yu., Latash, Yu.V. (1983) *Electroslag casting and refining of metals*. Kyiv: Naukova Dumka.
12. Rabkin, D.M., Ishchenko, A.Ya. (1970) On the results of pilot-industrial trials of aluminium alloys electroslag refining. *Tekhnologiya Lyogk. Splavov*, **6**, 14−16.
13. Lyuty, I.Yu., Latash, Yu.V., Krestianov, V.I. et al. (1974) Electroslag refining and modification of cast iron. In: *Advanced technological processes of cast iron melting and processing*. Penza: TsNTI.
14. Wolfgang, H., Harald, H., Bertram, O. (1993) Electroslag heating in tundish or ladle. *Steel Times*, March, 150−155.

NEW METHOD FOR DISPERSING THE MELT IN ELECTRON BEAM UNITS AND EQUIPMENT FOR ITS REALISATION

G.V. ZHUK and **N.P. TRIGUB**

The E.O. Paton Electric Welding Institute, NASU, Kyiv, Ukraine

New method for dispersion of the melt from a cold hearth during the electron beam remelting process has been developed. Technological fixture for its realisation in the electron beam furnace has been manufactured. The process of producing aluminium alloy AMg1 ingot by the new method is described. Macro- and microstructures of the resulting sample have been examined.

Key words: *electron beam unit, melt dispersion, rapid solidification, technological fixture*

Current metallurgical technologies provide for formation of structure and properties of metal at the stage of its melting. This allows subsequent technological costs related to thermomechanical treatment of ingots or castings to be minimised. This factor is especially important for multi-component alloys (high-temperature, heat-resistant, corrosion-resistant, etc.). The target in melting such alloys is to provide a refined structure and avoid structural and chemical macro- and microheterogeneity. One of the ways of achieving this target consists in increasing the number of crystallisation centres in solidification of the metal melt by raising initial cooling rates [1]. Under electron beam remelting conditions the metal cooling rate during solidification can be substantially increased by using the method for dispersion of the melt from the consumable billet surface [2]. The main drawback of this method is that it is necessary to preliminarily make a cylindrical billet and that the billet should meet high requirements for alignment and surface finish.

The E.O. Paton Electric Welding Institute has developed a new method for dispersing the metal melt directly from the cold hearth by using a rotary drum-type mould (divider) (Figure 1).

The point of the method is as follows. Melting of a consumable billet or a charge takes place in the electron beam unit like in electron beam remelting. Both bulk materials (scrap, sponge semi-finished products) and solid welded billets (in the case of alloying the base metal of an alloy) can be used as raw materials to be remelted. The consumable billet is fed by the feed mechanism to the melting zone, where it is melted under the effect of electron beams to flow to the cold hearth. A metal pool is formed in the cold hearth after building-up of the skull. The pool is maintained by heating with the scanning electron beams. Molten metal accumulated in the cold hearth is poured to the rotary drum-type mould, where it is built-on in the form of the skull to a required thickness. Then the drum-type mould is imparted a high rotation speed (about 2000 rpm), and the skull surface is melted by the concentrated electron beam. The molten metal is stripped under the effect of the centrifugal forces from the skull surface to flow along a line tangent to the focal spot of the concentrated electron beam in the form of a jet of dispersed liquid droplets. The jet of these droplets, having a small diameter (about 1 mm) and high speed (about 10 m/s), is directed to the forming surface (mould).
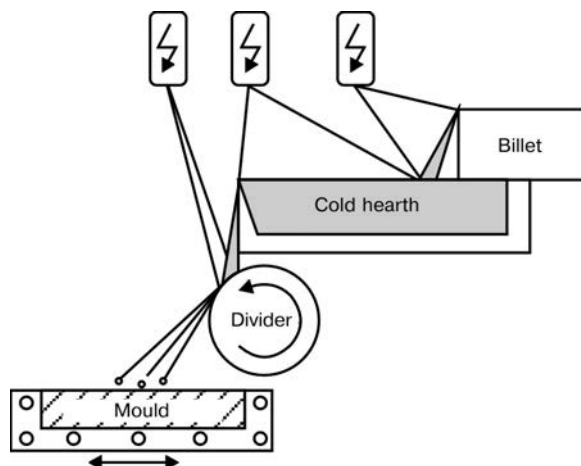

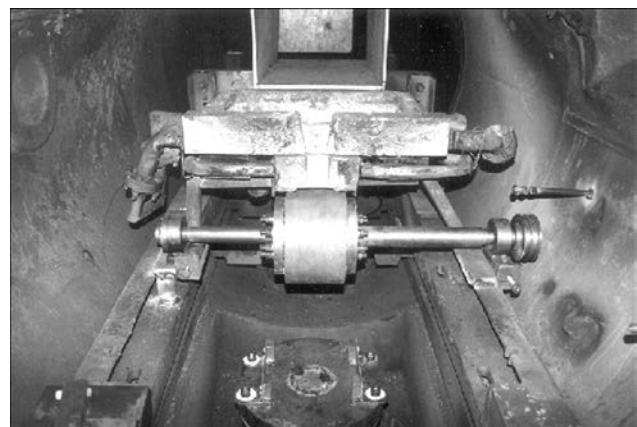**Figure 1.** Schematic of dispersion of the melt from the cold hearth

Figure 2. Technological fixture inside the work chamber

Figure 3. Upgraded electron beam unit UE-208

In the mould the droplets spread into a thin layer (≈ 0.1 mm thick) under the effect of the pressure head and solidify with no formation of the liquid pool. Water-cooled hearth (to produce ingots), metal plate (to produce bimetal compositions), groove of parts to be welded (for welding), or a frame of hardening elements (to produce composite materials) can be used as a mould.

The new method for dispersion from the cold hearth was realised using the upgraded unit UE-208 [3]. The dispersion mechanism is mounted on the unit. Physically, the mechanism consists of a dispersing drum-type mould with replaceable working surfaces (titanium, copper), system for imparting rotation using a vacuum-tight adapter, electric motor and control system.

The drum-type mould is mounted on the shaft using a special fixation system to minimise heat transfer from the working surface of the drum-type mould to the shaft. In turn, the shaft is secured in bearings on supports fixed on the frame of the unit (Figure 2). Three-phase asynchronous motor with a power of 2.2 kW is located outside the unit (Figure 3). Rotation is transferred from the motor to the drum-type mould using a flexible gear via the vacuum-tight sleeve built into the cooling jacket of the work chamber of the UE-208 unit. The rotation mechanism is controlled using the electronic system «Razmer». In this case the speed of rotation of the divider can be gradually regulated within a range of 0 to 2500 rpm. Connections are made in the ingot chamber of the unit to introduce thermocouples (3 pcs) into the melting chamber. The thermocouples used were tungsten-

Figure 4. Technological fixture mounted on a moveable frame: *1* — non-consumable box; *2* — cold hearth; *3* — drum-type mould
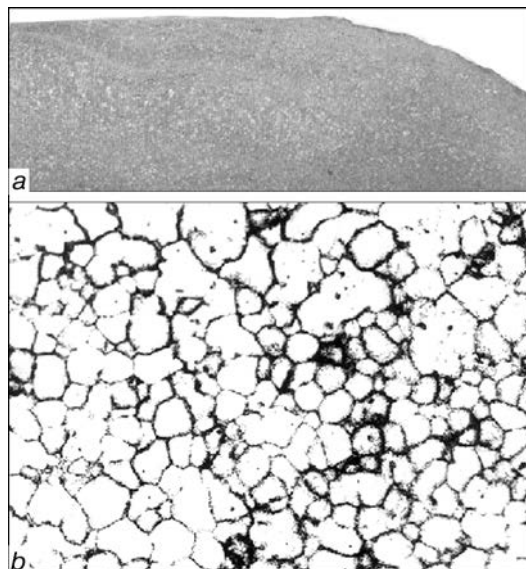

Figure 5. Macro- (*a*) and microstructure (*b*) ($\times 50$) of the AMg1 alloy sample produced by the melt dispersion method

rhenium and chromel-alumel ones. They were connected to the KSP-4 recorder. The mould (substrate), having horizontal openings to fix thermocouples, is installed on the hearth of the rod to withdraw ingots, which allows position of the mould relative to the dispersed flow to be regulated via vertical displacement of the rod.

Melting was done in compliance with the above procedure. Residual pressure during melting was as follows: 0.05 Pa in the melting chamber and 0.005 Pa in the electron beam heating chamber. Scrap of aluminium alloy AMg1 was used as the charge. The charge was fed from a non-consumable box into the cold hearth, from which the melt was poured to the drum-type mould (Figure 4). Distance from the cold hearth spout to the surface of the drum-type mould in vertical and horizontal directions, as well as the drum-type mould rotation speed were selected experimentally. This resulted in the formation of a jet of the dispersed melt droplets directed onto the substrate. The dispersion process was carried out until the ingot 40 mm thick was grown. Then the electron beam heating was stopped and cooling of the ingot was performed under vacuum conditions.

Chemical composition of the resulting sample was determined by the spectral analysis method, %: Al — base, 0.17Cu, 0.14Fe, 0.52Mg, 0.02Mn and 0.1Si. Macro- and microstructures of the cross section of the sample were examined (Figure 5). Macrostructure of the sample was fine-grained, containing no pores or discontinuities. Regions with a differing grain size, i.e. from 100 to 400 μm, were detected. Microstructure of the sample was heterogeneous, consisting of grains of α-solid solution and Mg_2Al_3 precipitates located along the grain boundaries.

1. Chalmers, B. (1968) *Theory of solidification*. Moscow: Metallurgiya.
2. Tikhonovsky, A.L., Pap, P.A., Kozlitin, D.A. et al. (1993) Electron-beam casting from dispersed melt. *Problemy Spets. Elektrometallurgii*, **3**, 35−39.
3. Tikhonovsky, A.L., Tur, A.A., Kravets, A.N. et al. (1992) UE-208 electron-beam unit. *Ibid.*, **1**, 71−74.

GROWING OF REFRACTORY METALLIC SINGLE CRYSTALS (REVIEW) *

V.A. SHAPOVALOV, M.L. ZHADKEVICH, G.F. TORKHOV, V.V. ZHOLUD and **V.V. YAKUSHA**

The E.O. Paton Electric Welding Institute, NASU, Kyiv, Ukraine

Basic methods of producing single crystals from refractory metal from vapour, liquid and solid phases are considered. Key attention was paid to the methods of producing crystals from the liquid phase: electron beam zone melting, plasma-arc drop melting, plasma-induction zone melting. It is shown that the technology of plasma-induction zone melting developed at the E.O. Paton Electric Welding Institute of the NAS of Ukraine is the most rational method of producing flat single crystal billets for further manufacturing of single crystal rolled metal (sheet, rods, wire).

Key words: single crystals of refractory metals, methods of growing single crystals, structure, shaped single crystal rolled metal

Major present and future scientific and technical programs of development of high technologies (space nuclear energy, aerospace engineering, chemical industry, etc.) depend greatly on the progress of science and engineering of refractory materials [1–3]. The solution of problems of producing functional materials possessing specific properties (ability of long-time operation under the conditions of high temperatures and aggressive media, cyclic loads and so on) becomes actual. Owing to the complex of unique physical and technological properties [4], typical of refractory single crystals, they satisfy greatly the requirements specified, therefore, they are the challenging materials named in the scientific-technical literature as functional materials. All these problems are inseparably linked with achievements of materials science, special metallurgy and rolled metal production in the technology of growing refractory metallic single crystals, their further processing and also in study of their properties.

In the natural form, the metallic single crystals are met in nature very rare, these are mainly crystals of noble metals (platinum, gold) [5]. Existing metals in a single crystal state were produced artificially. Brief history of appearance of main methods of their growing is given in [6].

At the stages of development and progress of the technology of growing single crystals, when the process is not automated or automated partially, the producing of single crystals with stable geometric sizes, preset crystallography, high degree of structural perfection and purity (at other conditions being equal) depend greatly on the skill (art) of an operator of the technological process.

Many existing methods of growing crystals, and they are more than 124 from the data of authors of [4], can be classified by several features. From the aggregate state of phases participating in the process of growth, the methods of growing single crystals from vapour, liquid and solid phases are distinguished. Each of this group of methods can be divided into subgroups. By the nature of heat energy sources methods with radiation, induction, electron-beam, plasma-arc, laser, solar and combined heat sources, and also electrolysis of melt of salts are distinguished.

Selection of either method of growing depends on characteristics specified for the single crystal. Analysis of methods of production of single crystals of refractory metals was made to study the feasibility of producing definite geometry of crystals, system of crystallographic orientations, degree of structural perfection and required level of purity of crystals being grown.

Growing of crystals from gas phase. Materials, produced by deposition from the gas phase, play a significant role in modern industry and their future wider application is expected. This is explained by that the deposition from gas phase is universal and comparatively economical method of a molecular forming (producing coatings, powders, products, instruments) by a controllable substance deposition in the form of separate atoms or molecules [7].

The process of growing single crystals from the gas phase found its development as far back as at the end of the XIX century. Mechanisms of growth of crystals from oversaturated vapour were described in many works devoted to the theory and practice of processes of growing single crystals [7–11]. Deposition from the gas phase can be defined as condensation of gaseous (vapour-like) elements or compounds with the formation of hard deposits. The gas phase can be of the same composition as the deposit. This is a usual case of a physical deposition from the gas phase at which the crystals are produced only due to the substance condensation. During chemical deposition from the gas phase its composition and composition of deposit are differed significantly from each other. In this case the deposits are formed as a result of chemical
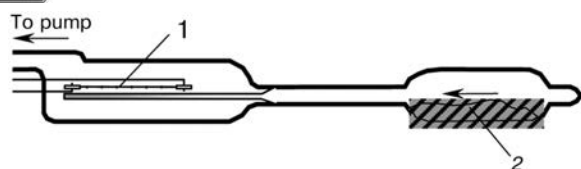
Figure 1. Scheme of growing tungsten crystal by the CTR method of van Arkel [8]: *1* — heated wire with tungsten priming «whiskers»; *2* — sublimated salt WBr5

reactions which are proceeding near the surface, at the surface or in a subsurface layer of a substrate.

Depending on the method of transporting the vapour-like substance from the source to the crystallization zone four main methods are distinguished [12]: molecular beams; cathode sputtering; crystallization from the gas phase in a closed volume; crystallization in the inert gas flow. Metal condensation may occur both into liquid and solid phases. Optimum temperature condition should provide the simultaneous existence of liquid and solid phases at hot and cold ends of the condenser. The large drawback of crystals grown by condensation from a natural vapour is the limited geometric sizes.

As regards to producing single crystals of refractory metals from the gas phase a method of chemical transport reactions (CTR) has found the most wide spreading [8, 13−17]. The schematic diagram of the method is shown in Figure 1. Single crystals produced in vapour deposition as a result of reduction of haloid salts (iodides, fluorides, chlorides, etc.) have comparatively large sizes and a required profile which is preset by the substrate surface geometry. The main factors influencing the nature of growth of crystals (surface morphology, structure homogeneity, growth rate and so on) are as follows: type of CTR, crystallography of substrate, value of pressure in a system, presence of adsorption-active gas components in the system (oxygen, fluorine, chlorine) [18, 19].

Single crystals of niobium, which were grown in the process of $NbCl_5$ hydrogen reduction on the heated niobium substrate (wire, strip) [14], had a disorientation of units of less than 0.5°. At certain conditions of conductance of experiments the single crystals of up to 12 mm length and 2−4 mm thickness were growing at separate areas of substrate. The growth of single crystals was observed mainly in the direction [111]. The essential drawback of crystals produced by hydrogen reduction is a high gas saturation. Content of gas impurities in niobium single crystals was in wt.%: 0.05H, 0.06N, 0.06O.

In works [15−19] the processes of producing and properties of gas-phase single crystal tungsten and molybdenum were selected as a subject of investigations. At sufficiently high degrees of oversaturation the single crystals of tungsten [18] deposited on molybdenum substrates had a homogeneous structure with macroscopically-smooth limited lateral surfaces. Depending on the structure of substrate, the presence of foreign impurities in it, pressure fluctuations in the system the substructures of different perfection were formed.

Using the CTR method the superthick (several millimeters) hexagonal single crystals of tungsten on

molybdenum single crystal tubular substrates of 10−20 mm diameter were grown in a chloride system [19] at the rates of growth up to 0.25 mg/(cm^2·s) at the following reaction on the substrate.

$$WCl_6 \xrightarrow{\;1700\,-\,1800\ K\;} W + 3Cl_2.$$
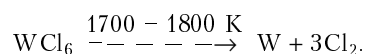
The CTR method is used widely for producing whiskers of refractory metals, as the comparatively long threads can be grown using a very simple equipment. The whiskers are characterized by a high internal perfection, have a more clearly expressed orientation, than the crystals grown by other methods, and, sometimes, very smooth facets of small indices [8].

When crystals are growing from vapour, there is a feasibility of a selective transition of initial material into the gas phase, next its transition to the substrate and producing deposit of a preset structure. Chemical transfer allows making an additional purification by a separating distillation of volatile intermediate products, and also by a selective reaction in the material source or on the substrate heated. Surfaces of the depositing single crystals are, as rule, very flat that is impossible to produce using other methods. Using CTR method it is possible to grow the quite pure crystals, however, it can be used only for metals which form volatile and easily-reduced compounds. This method makes it possible to attain the relatively high rates of crystal growth at temperatures being much lower than the metal melting points.

However the rate of growing single crystals from the gas phase is lower by several orders than the rate of growth of crystals from the melt due to a low concentration of the substance being crystallized in vapour. The single crystals produced from the gas phase have negligible sizes and increased content of gas impurities. It is not always managed to grow crystals of the preset shape and crystallography. The above-mentioned circumstances limit at present the wide application of gas-phase methods for growing single crystals of refractory metals. As a rule, these technologies find application for producing whiskers and thin epitaxial films.

Producing single crystals in solid phase. The application of methods, based on processes of recrystallization, are known long ago in the practice of growing of single crystals. The first information about producing single crystals using the method of «deformation-annealing» is referred to 1921 when Carpenter and Ilam first suggested this method for producing single crystals and large-crystalline aluminium [20]. In spite of their age, the solid-phase methods of crystal growing are used widely in industry. At present this is one of optimum possible methods of producing single crystals in the form of plates, strip and wire with rigid tolerances in geometry, and also single crystals with a wide interval of crystallization.

Conditions, at which the growth of single crystals in a solid phase is occurred, differ in the main from the conditions existing in the process of growth of crystals from melt or vapour. In the given case the surface of the growing crystal does not collide with free atoms and molecules and should capture particles

from the adjacent layers of the surrounding matrix having the crystalline structure. As a result, the growth of crystal occurs by a gradual movement of grain boundary between two differently oriented regions of the crystalline lattice [21].

Formation of single crystal structure in a solid state is associated with a dominating growth of one grain at the expense of a surrounding polycrystalline matrix. From the energy point of view, this process is more profitable, its motive force is the decrease in surface energy of grain boundaries due to decrease in their total extension and action of surface tension forces [22]. At some definite temperature the amplitudes of oscillations of atoms are increased so that their transition from one crystal to another becomes possible, i.e. the movement of grain boundaries is occurred.

The process of formation of a single crystal structure in heating of a semi-crystalline sample deformed to a critical degree is beginning from nuclei prone to the further growth. The growth of nuclei occurs due to transition of atoms from deformed crystals to more resistant thermodynamically smaller-deformed crystals. The first stage of recrystallization (primary or recrystallization of processing) consists in replacement of deformed grains by new undeformed grains. The second stage (collective recrystallization) results in growth of new small-deformed grains coming into contact with deformed grains. In a perfect case the collective recrystallization leads to occurrence of a stable single crystal structure of metal. However, this is difficult to attain in practice. One of the main causes of braking the grain growth is the impurities which are arranged along the boundaries [5]. This requires the use of the high-purity initial materials. The second direction providing the favourable growth of crystals is based on use of alloying microfillers [23—29] which stimulate the growth of grains in a solid phase. The presence of a dosed amount of calcium and manganese oxide brakes the normal growth of grain in the low-temperature region of annealing and promotes its anomalous growth in the high-temperature region [25].

According to these developments, the sintered billets are manufactured from the matrix metal (tungsten, molybdenum) with microadditions CaO and MgO by the method of a powder metallurgy and then subjected to the high-temperature plastic deformation (rolling with a high reduction ratio) to produce the primary texture. Formation of single crystal structure occurs in annealing of samples in vacuum or hydrogen during several dozens of hours at temperatures which are lower than the temperature of matrix metal melting. There is information about producing single crystal tungsten 140×100×60 mm plates using the above-mentioned technology. Single crystals containing alloying microadditions [24, 27] are characterized by the presence of high internal stresses. The microregions of other orientation, i.e. «parasitic» island grains, are remained usually in them.

In most methods of growing crystals a temperature gradient is created in heating [21] whose presence in the growth process is necessary to prevent the arbitrary origination of nuclei in different regions of the sample. The most favourable conditions for the growth are provided in that case when a nucleus is introduced into a furnace hot zone, which is growing so quickly that absorbs a fine-grain matrix before the origin of the second nucleus in it. Optimum gradient and rate of movement of the sample are determined by a temperature relationship of rates of origin and growth. This conclusion is based on the fact that the amount of grains which occurs in the sample is increased often with the increase in the heating rate.

As with all the existing methods of producing single crystals the present method has its advantages and disadvantages. Disadvantages include the complexity of control of orientations of the growing crystal, limitation of sample thickness, possibility of appearance of «parasitic» island grains of sizes from 0.05 to 0.10 mm in the single crystal structure [28] which disturb the monocrystallinity and deteriorate properties, make further processing by deformation more complicated, being centers of initiation of cracks leading to the crystal fracture. The basic drawback is the impossibility of producing single crystals of a definite crystallographic orientation as the processes of deformation in crystals are proceeding along the crystallographic planes and directions defined for each type of lattice [30].

However, the methods of producing crystals in a solid state are often more preferable than others by the following reasons: they allow us to produce single crystals in which the phase transformations are occurred between the melting point and room temperature; in combination with preliminary chemical cleaning the recrystallization annealing can provide producing single crystals with a sufficiently perfect structure characterized by absence of subgrains and relatively uniform density of dislocations; shape of sample can be more accurate than in growing from the melt, thus providing in some cases the easy producing of crystals in the form of thin sheets or wire of small diameter (method of Huger [31]).

Producing of single crystals of refractory metals by the method of electron beam zone melting (EBZM). Among the liquid phase methods of growing single crystals of refractory metals using the highly-concentrated heat sources, the EBZM occupies one of the first places in this field as to the industrial application, number of published scientific works and degree of study.

The method of a zone melting with electron heating has a number of advantages [32]: high specific concentration of power; high efficiency factor of units (more than 70 %); feasibility of creating a very narrow zone of heating by focusing the beam of electrons; feasibility of zone movement not only as a result of a mechanical movement of the sample or emitter, but also due to deflection of the flow of electrons.

The growth of crystals under the EBZM conditions is proceeding by the process of a directed crystallization of a slowly moving narrow zone of the molten metal. To avoid the contact of refractory metal being remelted with a crucible material and to prevent it from inevitable contamination, the process of growing single crystals is performed by vertical crucible-free EBZM (Figure 2). In a vertically-located sample a narrow molten zone of metal, formed by a beam of
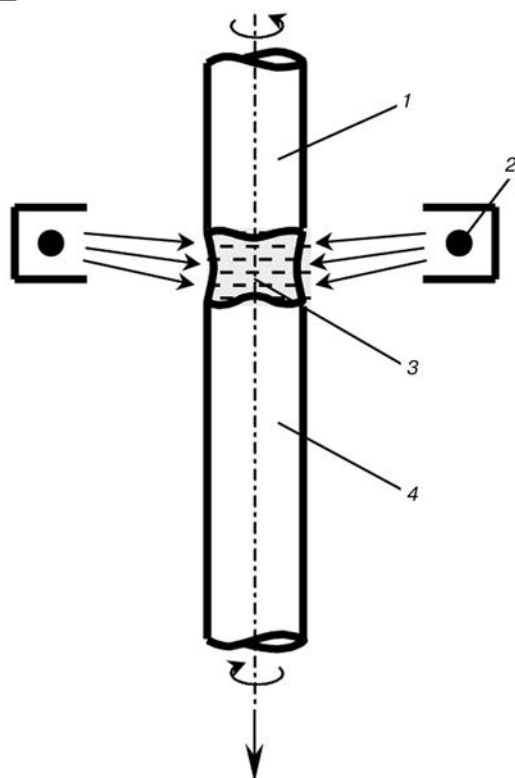
Figure 2. Scheme of crucible-free electron beam zone melting: *1* — polycrystal rod; *2* — annular cathode; *3* — «floating» zone; *4* — single crystal

electrons, is maintained from flowing out by surface tension forces. Here, the ratio of surface tension (in N/m) to melt density (in kg/m^3) should be not less than 100:1 [12]. The method makes it possible to grow single crystals of molybdenum and tungsten of a cylindrical shape (at through melting of the billet) of diameter up to 25 and 20 mm, respectively.

The installations for zone melting with an electron heating are divided into two basic classes by the type of electron emitters: with circular and axial emitters. The circular emitters are more often used in installations for the vertical crucible-free zone melting, as more economical and simple in design.

During the process of the crucible-free EBZM the intensive (burst) evaporation of impurities which is accompanied by spatters of the molten metal is possible. In parallel, the significant evaporation of the parent metal is also observed [33]. In this case, a simultaneous contamination of both cathode with evaporating admixtures and droplets of metal, and also of the remelting metal with a cathode material is possible, thus resulting in instability of anodic current influencing negatively on the quality of the crystal being grown. To avoid the above-mentioned, special designs of the cathode unit are made using shields and deflecting systems. The evaporation of admixtures and zone secondary recrystallization are the main mechanisms of refining refractory metals in EBZM [34, 35]. The high degree of refining is attained by a multiple movement of the molten zone along the ingot.

The electron melting is closely connected with the presence of vacuum. The experience shows that during operation of the installation for zone melting using electron heating the residual pressure in chamber should be not more than $1.33 \cdot 10^{-2}$ Pa. As a rule, the use of oil vacuum pumps does not provide the producing refractory single crystals with a low content of carbon. However, the single crystals of tungsten [36], grown from commercial rod tungsten under conditions of superhigh vacuum at a low ($6.66 \cdot 10^{-9}$ Pa) partial pressure of hydrocarbons (application of cryogenic condensation and sorption vacuum pumps), had high degree of purity and a low density of dislocations of $9 \cdot 10^3 - 1 \cdot 10^4$ cm^{-2} order. During zone melting the metallic impurities, close to the base element by vapour pressure, in particular of such refractory metals as vanadium, zirconium, are not almost removed and the refining from interstitial impurities is low-effective [34].

The use of integrated technologies including a deep refining of initial materials [37, 38] and next multiple EBZM gives an opportunity to grow single crystals of tungsten with molybdenum content and single crystals of molybdenum with tungsten content at the level of 1 ppm. The produced crystals are characterized by ratio of electric resistances $R_{300 \text{ K}}/R_{4.2}$, equal to 70,000 for tungsten and 100,000 for molybdenum. These high values of relative residual electric resistance give grounds to state [39] the structural perfection of the produced single crystals. Crystals of a small diameter (5−10 mm) have this structural perfection and high purity. The tungsten crystals, grown by EBZM, are characterized usually by the density of dislocations of $10^5 - 10^7$ cm^{-2} order and substructure of three scale levels. The main sources of dislocations are high thermal stresses existing both in growth and in cooling of single crystals.

Crystals of a large diameter (up to 55 mm) can be produced by the method of a periphery electron beam zone melting [32, 40, 41]. The periphery EBZM gives an opportunity to grow layer-by-layer the additional single crystal layers on a single-layer primer without a through penetration of the primer (Figure 3). There is a high probability in this process of an appearance of pores at the crystal−deposited layer interface. In the near-surface region, obtained by an increment of layers, a branch substructure directed at the angle to the surface is observed. Crystals are susceptible to cracking at pressure treatment as they have high internal stresses which are caused by high temperature gradients in the ingot section.

Producing of single crystals of refractory metals by plasma-arc method. Growing of single crystals of such refractory metals as tungsten, molybdenum, tantalum and others by a classical scheme of Verneuil method [42] was not realizable in principle. Temperatures which were attained using gas torches and high-frequency plasmatrons (maximum about 2800 °C) did not provide melting and maintenance of the mentioned metals in a molten state. General tendencies of development of the plasma metallurgy at the middle of the last century and development of low-temperature plasma sources of a high unit power promoted the further development of the Verneuil method for producing high-temperature metallic crystals.

Technology of crucible-free plasma-arc drop melting (progress of the Verneuil method) was a progressing alternative to the EBZM process and gave a fea-

sibility to increase both geometric sizes and also number of geometric shapes of crystals being melted. The data about producing refractory metallic crystals both by domestic and foreign scientists appeared almost simultaneously in the scientific-technical literature [43, 44].

Plasma-arc heating as regards to growing single crystals of refractory metals can melt and maintain a comparatively large volume of metal in a molten state, create a gaseous atmosphere of a preset composition and pressure in the melting chamber that differed it beneficially from the EBZM melting [45].

The plasma-arc technology in production of refractory single crystals, developed by scientists of A.A. Bajkov Institute of Metallurgy of the Russian Academy of Sciences (IMET RAS) in 1968 under supervision of Savitsky E.M. and Burkhanov G.S., was developed rapidly during recent years. Based on the investigations, the laboratory and industrial installations of plasma-arc heating were manufactured, producing crystals both in the form of a cylinder and in the form of pipes of a variable section and small plates. The sizes of produced crystals more than twice increased the sizes of crystals produced by conventional EBZM. Tungsten and molybdenum crystals of 50 and 65 mm diameter, respectively, were melted by the mentioned method.

In the method considered the growing of crystals is started from fusion of an edge surface of the primer by a plasma jet (Figure 4) [46]. Then, the continuous adding of a pool is made by a lateral feeding of the rod and its fusion in a plasma jet. Simultaneously, the primer, located on a pin, is displaced downward keeping the interface of liquid-solid phases at a constant level.

Later the technological diagrams were tested in which refractory powder-like particles, directly fed into a plasma jet were used instead of consumable rods. Due to a high area of powder material reacting with a plasma arc the processes of refining of the crystals being grown are proceeding more intensively. There is no need in labour-intensive preliminary stage of producing remelting rods by sintering rod pieces with a subsequent operation of a rotational forging [31].

As compared with electron beam method the plasma-arc method using argon with helium additions as a plasma gas provides more effective removal of carbon, oxygen, silicon, phosphorus, sulphur, chromium, manganese, iron, nickel, aluminium and other impurities from tungsten. The removal of impurities occurs in fusion of an initial billet, from a drop of melt and from the melt directly [47]. Content of carbon in tungsten single crystals does not exceed 0.002–0.005 %.

When melting single crystals of large sizes it is necessary to maintain large masses of metal in a molten state to have a continuous adding of crystal during growth. In the given method this is attained by using plasmatrons of a special design, which form a plasma jet with a temperature in the periphery zone equal to the temperature of metal crystallization. Due to overheating of central regions of metal pool with respect to its edges a concave front of crystallization is formed [48], which can maintain a large volume of molten metal at the edge of the single crystal being grown
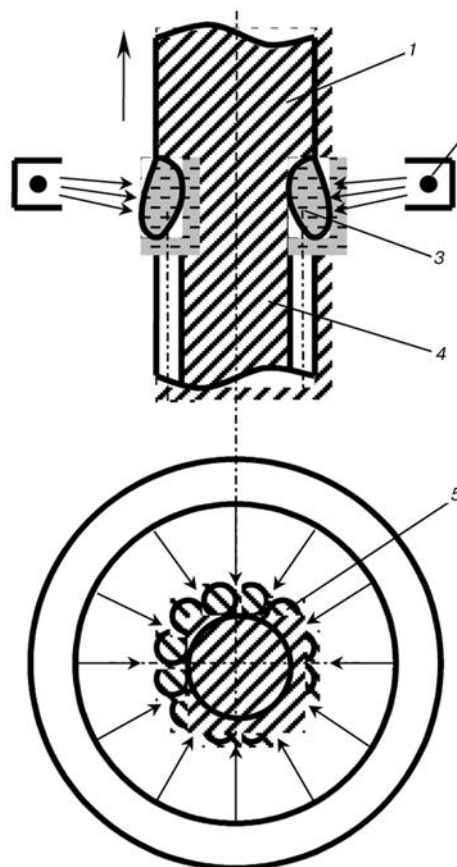

Figure 3. Diagram of growing single crystals using the method of a periphery electron beam zone melting [32]: *1* — single crystal; *2* — annular cathode; *3* — «floating» zone; *4* — single crystal bar-primer; *5* — bundle of rods remelted

from flowing. However, the increase in curvature of crystallization front, from the other side, leads to a growth in number of forming defects in a solid phase near the front of crystallization. Crystals which were grown by the plasma-arc method, are characterized by a developed structure, forming under the action of non-homogeneous temperature fields and high radial and axial gradients of temperatures. The mean density of dislocations of single crystals of tungsten and molybdenum is at the level of 10^6–10^7 cm^{-2}.

Quality of a lateral surface of crystals depends greatly on stabilization of electric parameters of a plasma source of heating and it is not satisfactory in some cases that complicates the subsequent processing of crystals in plastic deformation (rolling, drawing, etc.).

Producing of refractory single crystals using the method of plasma-induction zone melting (PIZM). Coming from the above-said it can be stated that the shaped single crystal billets for wide-sized rolled metal can be produced using the methods of a secondary recrystallization or the technology of plasma-arc drop melting. Due to specifics in growing refractory single crystals by the mentioned methods the initial billets do not always meet the requirements for the crystallographic orientation, degree of structural perfection and purity, specified by the conditions of the rolling process. A rectangular plate is the most optimum shape of the billet for its further rolling into a wide-sized sheet or foil.
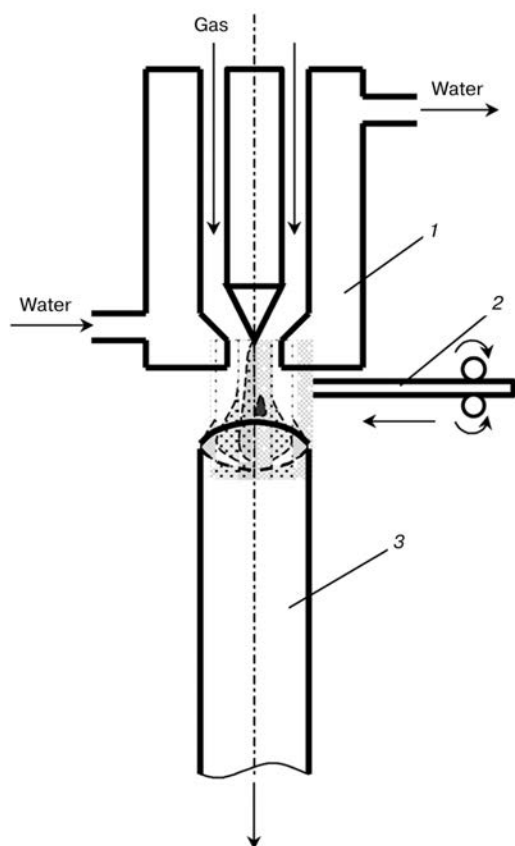
Figure 4. Diagram of growing single crystals of refractory metals using plasma-arc heating [4]: *1* — plasmatron; *2* — rod; *3* — crystal

Manufacture of products from crystals with a guaranteed preserving of a monocrystallity after a high plastic deformation and effect of high temperatures is one of the most important problems of high technologies of refractory metals for special applications [44]. Tungsten slabs of 9.5×38×305 mm size, suitable for deformation, were manufactured using the plasma-arc technology, developed by the authors of this work. There is available information about producing single crystal plates of molybdenum of 8×75×160 mm size using the method of IMET RAS [4].
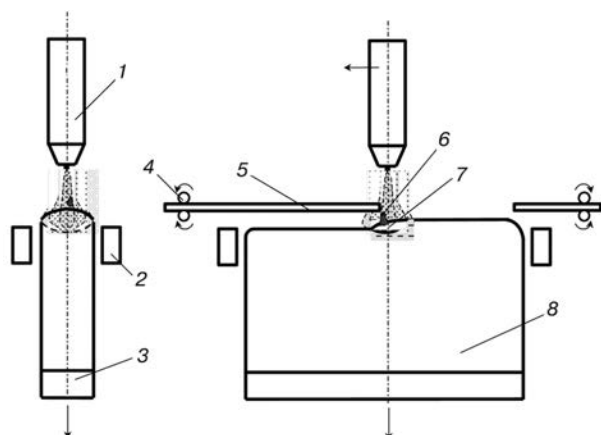
Figure 5. Diagram of plasma-induction method of growing profiled single crystals of refractory metals of the PWI [49]: *1* — plasmatron; *2* — inductor; *3* — priming crystal; *4* — mechanism of rod feeding; *5* — rod; *6* — molten metal drop; *7* — molten metal pool; *8* — crystal

At the beginning of the 1980s of last century the scientists of the PWI developed the technology of producing single crystals using the method of a PIZM under the supervision of Yu.V. Latash, G.M. Grigorenko and Yu.M. Pomarin [49]. This was a great progress in the field of technologies of growing large single crystals of refractory metals. Using this technology the oriented single crystal cylindrical samples of more than 20 mm diameter and also plates of 20×140×170 mm size, made from molybdenum and tungsten, were produced.

A radical difference of this technology from the plasma-arc technology consisted in use of an independent source of induction heating, fulfilling the functions of an additional heating of growing crystal. This made it possible to decrease significantly the temperature gradients in its section and to produce a single crystal ingot suitable for further deformation without a risk of its fracture.

The process of single crystal growing consists of a layer-by-layer increment of metal on the oriented single crystal primer under the conditions of heating of a forming part of the crystal by a high-frequency electromagnetic field (Figure 5). Helium-argon mixture with helium content up to 70 % is used as a plasma gas. Unlike the plasma-arc technology the metal pool in PIZM is maintained from flowing by surface tension forces and also electromagnetic field of HF inductor. A rigid stabilizing of geometric parameters of the crystal is attained by an adjustable change in power of plasma-arc and induction heat sources during melting, thus avoiding the formation of rough defects (overlaps, spillages) that is important at its further pressure processing. In the mentioned heat conditions of PIZM the profile of a crystallization front is formed which is close to a plane profile with a negligible concave central part and convex edges [50]. In case of a parasitic crystal, resulted from random heat fluctuations in the process of single crystal growth, the above-mentioned shape of the crystallization front will not only prevent the defect deepening inside the body, but also promote its escape to the ingot surface. The same as in the plasma-arc technology, a significant reduction of carbon concentration in the single crystal tungsten (down to 0.0005 %) is attained due to the presence of a controllable gas atmosphere. Oxygen content is at the level of 0.0008, nitrogen — 0.002 % [51].

The X-ray examination of substructure of PIZM-crystals showed that they are solid single crystal bodies with an orientation of facets which corresponds to the preset priming crystals with possible deviations from the growth axis up to 3°. The density of dislocations is $1-5\cdot10^6$ cm^{-2}.

The preliminary investigations of deformed single crystal billets showed that they can be used for producing profiled single crystal rolled metal of refractory metals [52].

Automation of the technological process of PIZM, which is at the stage of a practical realization, gives grounds to expect the real increase in the quality of ready single crystal products and the process productivity.

In can be concluded from the above-described review of major methods of production of single crystals of refractory metals that the methods of growing crystals from solid and liquid phases have the most wide practical application. Technically-complicated and actual problems of producing shaped single crystal billets find the most complete and effective solution in use of the plasma-induction technology of growing refractory single crystals, developed at the E.O. Paton Electric Welding Institute of the NAS of Ukraine.

1. Schider, S. (1988) Hochschmelzende Metalle fuer High Tech-Anwendungen. *Metall: Internationale Zeitschrifte fur Technick und Wirtschaft*. Berlin-Heidenberg: Metall.
2. Wittenauer, J. (1990) Refractory metals 1990: old challenges, new opportunities. *JOM*, **8**, 7.
3. Briant, C.L. (1999) Processing refractory metals: the traditional and the novel. *Ibid.*, **4**, 28.
4. Burkhanov, G.S., Shishin, V.M., Kuzmishchev, V.A. et al. (1981) *Plasma growing of refractory single crystals*. Moscow: Metallurgiya.
5. Savitsky, E.M., Burkhanov, G.S. (1972) *Single crystals of refractory and rare metals and alloys*. Moscow: Nauka.
6. Cahn, R.W. (1999) The use of metallic single crystals in metals research: a concise history. *Metallkde*, **11**, 860.
7. (1970) *Gas phase deposition*. Ed. by C. Powell, K. Ocksly, J. Blocher. Moscow: Atomizdat.
8. Brenner, S.S. (1968) *Theory and practice of single crystals growing*. Moscow: Metallurgiya.
9. (1963) *Processes of growth and growing of single crystals*. Ed. by N.N. Sheftal. Moscow: Inostr. Literatura.
10. (1977) *Growth of crystals. Theory of growth and methods of growing of single crystals*. Ed. by K. Gudman. Moscow: Mir.
11. Ivanov, V.E., Nechiporenko, E.P., Krivoruchko, V.M. et al. (1974) *Solidification of refractory metals from gas phase*. Moscow: Atomizdat.
12. Lyakishev, A.P., Burkhanov, G.S. (1995) Single crystals of materials with metal type of compound. *Vysokochist. Veshchestva*, **1**, 5–17.
13. Evstyukhin, A.I., Abanin, D.D., Maslov, V.P. (1973) Producing and properties of chrome single crystals. In: *Growing of single crystals of rare and refractory metals*. Ed. by E.M. Savitsky. Moscow: Nauka.
14. Petrusevich, I.V., Abramov, V.V., Firsov, V.I. et al. (1973) On producing of niobium single crystals in reduction of $NbCl_5$ from vapour phase with hydrogen. *Ibid*.
15. Sidorov, Yu.I., Rymashevsky, G.A., Smirnov, V.P. et al. (1987) Producing of tungsten single crystal plates by solidification from gas phase. In: *High-purity and single crystal metallic materials*. Ed. by A.I. Manokhin. Moscow: Nauka.
16. Smirnov, V.P., Yanchur, V.P., Sidorov, Yu.I. et al. (1987) Morphology and structure of gas-phase single crystal tungsten. *Ibid*.
17. Karetnikov, D.V., Koryukin, V.A., Obrezumov, V.P. (1987) Emission properties of gas-phase chloric tungsten of cylindrical shape. *Ibid*.
18. Reitzenstein, W., Weise, G. (1971) Die Realstruktur von aus der Gasphase gewachsen Molybdän- und Wolframeinkristallen. *J. Crystal Growth*, **5**, 228–237.
19. Kobyakov, V.P. (1996) Facetting of tungsten precipitates during gas-phase epitaxy on cylindrical surface of substrate Mo <111>. *Kristallografiya*, **3**, 552–556.
20. Gorelik, S.S. (1978) *Recrystallisation of metals and alloys*. Moscow: Metallurgiya.
21. Burgers, V.G. (1968) Main notions concerning recrystallisation. In: *Theory and practice of growing of single crystals*. Moscow: Metallurgiya.
22. Savitsky, E.M., Burkhanov, G.S., Povarova, K.B. et al. (1986) *Refractory metals and alloys*. Moscow: Metallurgiya.
23. Fujii, T., Okamoto, K. (1989) Effect of dopants on the secondary grain growth in the hot-rolled tungsten sheet. *J. Jap. Soc. Powder and Powder Met.*, **7**, 819–823.
24. Kato, M., Iida, S., Sugita, H. et al. (1991) X-ray characterization of tungsten single crystals growth by secondary recrystallization method. *J. Crystal Growth*, **2/3**, 368–372.
25. Fujii, T., Watanabe, R., Hiraoka, Y. et al. (1984) Preparation of large-scale molybdenum single crystals sheet by means of secondary recrystallization. *J. Less-Common Metals*, **1**, 297–304.
26. Takeba, K., Fujii, T. (1989) Preparation of large-scale molybdenum bicrystals sheet from sheet Mo by means of secondary recrystallization. *J. Jap. Soc. Powder and Powder Met.*, **3**, 284–291.
27. Hiraoka, Y., Kuo, C.L., Billelo, J.C. (1989) Perfection of molybdenum single crystal produced by means of secondary recrystallization. *J. JIM*, **10**, 1077–1078.
28. Hiraoka, Y., Ei-ichi Sukedai (1994) Room temperature slip in molybdenum bicrystal prepared by means of secondary recrystallization. *Metallkde*, **4**, 232.
29. Fujii, T., Hiraoka, Y., Watanabe, R. *Large crystals grains or single crystals of molybdenum and process for production thereof*. Pat. 4491560 USA, Int. Cl. C22C 27/04; C22F 1/18. Publ. 07.01.85.
30. Zolotarevsky, V.S. (1983) *Mechanical properties of metals*. Moscow: Metallurgiya.
31. Smitells, C. (1958) *Tungsten*. Moscow: Metallurgiya.
32. Ratnikov, D.G. (1976) *Crucible-free zonal melting*. Moscow: Metallurgiya.
33. Brodsky, I.A., Krokhmalev, V.A., Petushkov, E.E. et al. (1973) *Single crystals of molybdenum and tungsten*. Tashkent: Fan.
34. Azhazha, V.M., Kovtun, G.P., Tikhinsky, G.F. (2000) Production and metallophysics of superpure metals. *Metallofizika i Nov. Tekhnologii*, **2**, 21–35.
35. Pfann, V. (1970) *Zonal melting*. Moscow: Mir.
36. Katrich, N.P., Pugach, G.M., Rozenberg, T.B. (1976) Examination of spectral distribution of residual gases in growing of tungsten single crystals in superhigh vacuum. In: *Metallic single crystals. Production and study of properties*. Ed. by E.M. Savitsky. Moscow: Nauka.
37. Kopetsky, Ch.V., Plyushcheva, S.V., Satunkina, L.F. et al. (1981) Producing of superpure tungsten. *Metally*, **2**, 59–81.
38. Klimenko, G.L., Blokhin, A.A., Glebovsky, V.G. et al. (2001) Application of ion exchange method in technology of production of high-purity tungsten and molybdenum. *Ibid.*, **3**, 49–51.
39. Tagirova, D.M., Dyakina, V.P., Startsev, V.E. et al. (1997) Structural perfection and residual electric resistance of tungsten single crystals. *Fizika Metallov i Metallovedenie*, **6**, 37–47.
40. Mikhajlov, S.M., Chechentsev, V.N., Shmakov, A.M. (1973) Experience of producing of non-porous molybdenum single crystals of increased diameter. In: *Growing of single crystals of refractory and rare metals*. Ed. by E.M. Savitsky. Moscow: Nauka.
41. Chernyshov, A.I., Shishkov, V.V., Dolomanov, L.A. (1987) *Study of substructure of increased diameter molybdenum single rystals*. Ed. by A.I. Manokhin. Moscow: Nauka.
42. Bayer, V.Kh., Fild, V.G. (1968) Verneil method. In: *Theory and practice of single crystals growing*. Moscow: Metallurgiya.
43. Savitsky, E.M., Burkhanov, G.S., Baranov, L.G. et al. *Method of production of single crystals of refractory metals and alloys*. USSR author's cert. 232214. Bull. Izobret., 12, 237.
44. Raymond, L., Carvat, F. (1966) Sheets from single crystal tungsten. *Raketnaya Tekhnika i Kosmonavtika*, **5**, 161–166.
45. Zhadkevich, M.L., Shapovalov, V.A., Shejko, I.V. et al. (2001) Study of technological parameters of plasma-induction melting of refractory metals single crystals. *Problemy Spets. Elektrometallurgii*, **4**, 27–31.
46. Savitsky, E.M., Burkhanov, G.S., Bondarenko, K.P. et al. (1977) Development of plasma methods of growing of single crystal refractory metals and alloys. In: *Single crystals of refractory and rear metals, alloys and compounds*. Ed. by N.V. Tinanaev. Moscow: Nauka.
47. Devyatykh, G.G., Burkhanov, G.S. (2001) High-purity metallic materials. In: *Proc. of 7th Int. Symp. on Pure Metals*. Kharkov.
48. Burkhanov, G.S., Kuzmishchev, V.A., Sdobyrev, V.V. (1987) Influence of some solidification parameters on perfection of tungsten single crystals structure produced by plasma-arc process. In: *High-purity and single crystal metallic materials*. Ed. by A.I. Manokhin. Moscow: Nauka.
49. Shapovalov, V.A., Kovalenko, A.A., Latash, Yu.V. et al. (1993) Investigation of process of growing of flat tungsten and molybdenum single crystals. *Problemy Spets. Elektrometallurgii*, **1**, 79–82.
50. Shapovalov, V.A., Zhadkevich, M.L., Torkhov, G.F. et al. (2002) Refining of tungsten in plasma-induction melting of single crystals. In: *Proc. of 8th Int. Symp. on High-Purity Metallic and Semiconductor Materials*. Kharkov.
51. Shapovalov, V.A., Zhadkevich, M.L., Torkhov, G.F. et al. (2002) Influence of heating methods on shape of interface in growing of coarse single crystals of refractory metals. *Ibid*.
52. Shapovalov, V.A. (2000) Application of plastic working of tungsten single crystals for wire manufacturing. In: *Transact. on Improvement of Processes and Equipment for Plastic Working in Metallurgy and Mechanical Engineering*. Kramatorsk.

THERMAL FIELD OF TUNGSTEN SINGLE CRYSTAL IN PLASMA-INDUCTION ZONE MELTING

V.A. SHAPOVALOV

The E.O. Paton Electric Welding Institute, NASU, Kyiv, Ukraine

Mathematical model has been selected for study of thermal fields of single crystals during heating with different sources: plasma-arc, high-frequency and combined plasma + high-frequency. It is shown that the combined heating makes it possible to control the curvature of phase interface. Under certain conditions the surface can become almost plane. The highest efficiency of the thermal field control is attained when all the crystal is heated by an inductor.

Key words: *tungsten, single crystal, plasma-induction heating, thermal field, modelling*

The method of plasma-induction zone melting (PIZM) for growing large oriented single crystals of tungsten and molybdenum, described in [1−3], has an indisputable advantage over other known methods. From the one hand, this is the use of the electromagnetic field to maintain a metal pool from flowing, and, from the other hand, the creation of the required thermal field in a growing crystal. During the period of development of the method the problem of a single crystal preheating was studied, but it was very difficult to determine the specific and total power of preheating, as there was no experience in realization of similar hybrid processes. Therefore, it was necessary to evaluate the effect of each heat source on the thermal state of the single crystal for the creation of a real process.

To solve the problem using a mathematical model, let us consider a definite scheme of a plasma-induction method of zone melting used for the single crystal growing. The method is peculiar by that the plasmatron, inductor and single crystal are coaxial and the axis is located vertically. The inductor can be composed of any number of turns, but the zone of its effect on crystal is limited by a height, which is not exceeding the diameter of the latter. Figure 1 shows the scheme of the PIZM process.

Modelling will be based on the solution of a non-stationary two-dimensional equation of heat conductivity in coordinates (r, z) [4]:

$$pc_V \frac{\partial T}{\partial \tau} = \frac{1}{r} \frac{\partial}{\partial r} \left(r \lambda \frac{\partial T}{\partial r} \right) + \frac{\partial}{\partial z} \left(\lambda \frac{\partial T}{\partial z} \right), \qquad (1)$$

where τ is the current time; T is the current temperature; $p = p(T)$ is the metal density; $c_V = c_V(T)$ is the isochoric heat capacity; $\lambda = \lambda(T)$ is the coefficient of metal heat conductivity. Solution of the equation of heat conductivity is impossible without definiteness in description of boundary and initial conditions [5].

Initial condition is

$$T \big|_{\tau = 0} = T_0, \qquad (2)$$

where T_0 is the temperature of environment with which the body is in contact.

Boundary conditions:
• the condition below is always fulfilled on the crystal axis

$$-\lambda \frac{\partial T}{\partial \tau} \big|_{r = 0} = 0, \qquad (3)$$

which is followed from the problem symmetry;
• over the entire surface S (except that covered with plasma) the heat losses by radiation Q_l and convection Q_c are linked by the following relationship:

$$-\lambda_a \nabla T \big|_S = Q_l + Q_c, \qquad (4)$$

where $a = m, h$ is the metal state (m — melt, h — solid body); $T \big|_S$ is the temperature in any point at the cylinder surface. Gradient of temperatures near surface (inside) of metal is determined along $\overrightarrow{n}$ unit vector, directed normal (outside) to surface; $Q_l = \sigma(\eta_S T^4 \big|_S - T^4)$, here σ is the Stefan−Boltzmann constant; η_S is the coefficient of surface dullness; $Q_c = k_n(T_S - T_0)$, where k_n is the coefficient of external heat conductivity which is quite empiric in accordance with Newton's law;
• at surface S_i the energy supplied from inductor is converted into heat flow Q_i per time unit:

$$-\lambda_a \nabla T \big|_S = Q_l + Q_c - Q_i. \qquad (5)$$

Sign «minus» in front of Q_i denotes that the flow is directed inside the body (in opposite direction with respect to $\overrightarrow{n}$).

In plasma-arc heating, to determine the heat exchange in the zone of arc action we shall come from the following:
• heat flow from plasma-arc source enters the single crystal through its upper edge. This heat flow is resultant and accounts for heat transfer from arc by convection and radiation, heat in arc anodic spot, heat coming for vapour formation, heat evolved in conden-

sation of metallic vapour at the pool surface and heat losses by the metal pool into furnace working space;

• distribution of heat flow density at the single crystal edge heated by plasmatron is preset by the equation

$$\begin{cases} q = Q; & r = 0, R_a; \\ q = h_1 Q; & r = R_a, R_l, \end{cases} \quad (6)$$

where q is the specific heat flow entering the metal in the zone of arc heating; Q is the specific heat flow entering the metal in the arc spot zone; h_1 is the normalizing factor; R_a is the arc spot radius, R_l is the metal pool radius;

• at the surface on which the arc spot is supported in region $S_a \, T\big|_S = T_b$, where T_b is the boiling temperature;

• at the surface of phase transition G_m the following equality is fulfilled:

$$-\lambda_h \nabla T \big|_{G_{m+h}} + \lambda_l \nabla T \big|_{G_{m+l}} = -E_m v_m, \quad (7)$$

where λ_l, λ_h are the coefficients of heat conductivity of liquid and solid phases, respectively; E_m is the melting energy; v_m is the rate of interface movement.

Combination of two heat sources changes the mode of heat transfer in the single crystal as a whole. Taking into account that each of the sources forms its thermal fields in the single crystal with a maximum generation of energy in different regions it can be assumed that this combination of sources will allow us to provide a flexible control of interface configuration between the solid and liquid phases. Configuration of interface, i.e. the crystallization front surface, will change from convex to concave. The configuration of interface will depend, from the one hand, on ratio of power of sources, and, from the other hand, on the conditions of heat exchange of single crystal with environment.

Heat processes will be studied on models corresponding to a real tungsten single crystal of 20 mm diameter and more than 100 mm length. Due to limitations, the model will provide only the approximate evaluation of the real process. First of all, these limitations are due to conformity of the model shape to
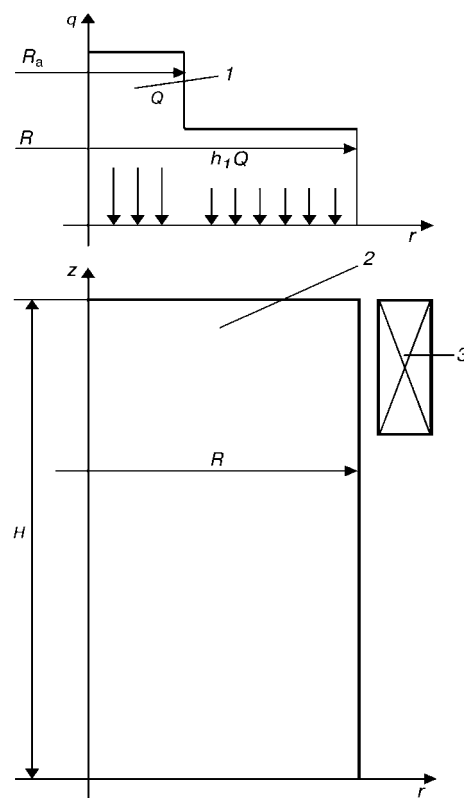
Figure 1. Scheme of a combined heating of a single crystal: *1* — heat flow from plasmatron; *2* — single crystal; *3* — inductor coil; R_a — arc spot radius; R — single crystal radius; h_1 — normalizing factor; H — height of single crystal; Q — specific heat flow in arc spot

the real crystal shape. In the real crystal the edges of the metal pool are rounded by the surface tension forces, while the pool edges of the model have an angle. Radius and angle influence on heat exchange processes in this region in a different way. Microregion, enclosed into angle, dissipates heat more intensively into surrounding medium. This influences the pool depth and shape of phase interface. Nevertheless, the use of even non-perfect model enables us to study the effect of each heat source on the formation of phase interface (crystal substructure).

To study the effect of each heat source on the distribution of temperatures in a single crystal, let us
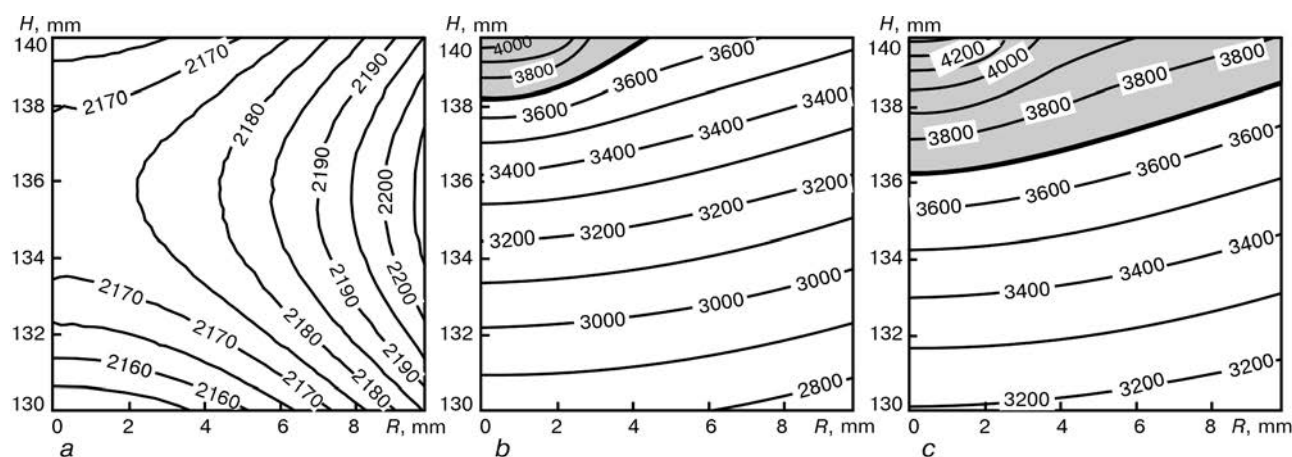
Figure. 2. Pattern of thermal field in upper part of single crystal in heating with different sources: *a* — inductor; *b* — plasmatron; *c* — inductor + plasmatron
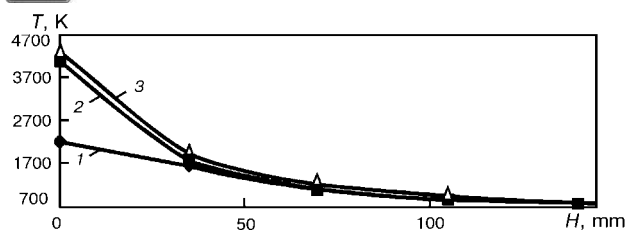
Figure 3. Distribution of temperature along the axis of single crystal in heating with different sources: *1* — inductor; *2* — plasmatron; *3* — inductor + plasmatron

consider the pattern of thermal fields. Figure 2, *a* and *b* shows thermal fields in heating crystal by one of the sources, i.e. by inductor and plasmatron, respectively. Power of each of sources is the same as in use of a combined heating. Therefore, it is difficult to form pool by plasmatron only or to melt tungsten by inductor only, but it is possible to create a definite temperature field. The lateral surface of the single crystal in the zone of inductor action is heated most intensively. Temperature of heating can be adjusted. Plasmatron heats the edge surface of the crystal more intensively, thus melting metal, but the pool is small, and the configuration of phase interface is distorted. Unfavourable conditions are created for the formation of the single crystal substructure.

Figure 2, *c* shows pattern of heating the upper part of the single crystal using a combined heating. Surface of the phase interface becomes more and more plane. The superposition of thermal fields of two heat sources creates perfect conditions for the structure formation. However, this is one aspect of the problem of formation of a thermal field of a growing crystal. The second aspect is the distribution of temperature along the axis of the single crystal growing. This is shown visually in Figure 3. Curves correspond to dif-

ferent conditions of heating: inductor heats the upper part of the single crystal, plasmatron heats the crystal from the edge, while in use of a combined source the plasmatron heats the single crystal from the edge, and the inductor heats its lateral surface.

It follows from the Figure that the effect of the combined heating on that part of the crystal which is located closer to its lower edge, differs negligibly from the variant of heating which is realized by one source, either inductor or plasmatron. Distribution of temperature in the single crystal does not depend on the type of heating at the distance from the upper edge of more than 2.5−3 diameters of a single crystal. It follows from the results obtained that to provide an effective control of single crystal temperature field it is necessary to use an inductor whose heating zone will cover all the lateral surface of the single crystal.

Thus, the combined heating using plasmatron and inductor makes it possible to change the configuration of interface of liquid and solid phases. Control of temperature field of the single crystal can be effective if to use the inductor which will heat all the lateral surface of the crystal.

1. Shapovalov, V.A., Kovalenko, A.A., Latash, Yu.V. et al. (1993) Study of process of tungsten and molybdenum flat single crystals growing. *Problemy Spets. Elektrometallurgii*, **1**, 79−82.
2. Shapovalov, V.A., Latash, Yu.V., Zholud, V.V. et al. (2001) Large-sized flat single crystals of tungsten and molybdenum and producing methods. In: *Proc. of 7th Int. Symp. on Pure Metals*. Kharkov.
3. Shapovalov, V.A., Latash, Yu.V., Borimskaya, S.T. et al. (2001) Oriented tungsten single crystals: producing, study and application. *Metally*, **1**, 60−64.
4. Isachenko, V.P., Osipova, V.A., Sukomel, A.S. (1981) *Heat transfer. Manual for higher educational institutions*. 4th edition. Moscow: Energoizdat.
5. Samarsky, A.A. (1987) *Introduction to numerical calculation methods*. Moscow: Nauka.

SPECIAL ELECTROMETALLURGY
AT THE BEGINNING OF THE XXI CENTURY[*]

B.E. PATON and **L.B. MEDOVAR**

The E.O. Paton Electric Welding Institute, NASU, Kyiv, Ukraine

An attempt was made to estimate the state-of-the-art and prospects of ferrous metallurgy, including the special electrometallurgy. The step, jumpy nature of the development of metallurgical technologies over the recent decades is shown. A conclusion predicts the approaching next period of a rapid updating of major metallurgical technologies.

Key words: *electroslag remelting, vacuum-arc remelting, superalloys, titanium, intermetallics*

The term «special electrometallurgy» was suggested at the PWI at the middle of the 1960s of the last century. The appearance of this term was due to the origin of a new subbranch of the ferrous metallurgy, specialized in a large-scale production, in hundred thousands tons of steels and alloys of superhigh quality on the basis of remelting processes, electroslag and vacuum-arc processes in particular. Let us define one linguistic point. In Russian and Ukrainian languages the word «special» has a nuance, directly indicating the relation of something or somebody to the military subject. At the same time the English equivalent «special» has a direct relation to high quality or a special position, in our case of metal in particular. For example, INKO Company, the world-known manufacturer of superalloys, is included now to Consortium «Special Metals». Thus, in Russian, Ukrainian and English languages the term «special electrometallurgy» describes exactly the production and fields of application of the metal of the highest quality.

Methods of special electrometallurgy both in our country and abroad include, except the above-mentioned ESR and VAR methods, a vacuum-induction melting, and also all varieties of plasma and electron-beam metallurgical technologies and, consequently, production of not only steel and superalloys, but also other structural materials, including titanium alloys, intermetallics and others.

Nevertheless, even today the special metallurgy is closely related to the ferrous metallurgy. The rapid development of both vacuum and other means of ladle treatment and their application in production of steels and alloys of the highest quality has led to the change in concept «special electrometallurgy». For example, at present there is no need to subject high-strength and ball-bearing steels to ESR, and nickel superalloys are passing often through AOD without vacuum-induction furnace. In this connection during recent years the term «special metallurgy» is used sometimes in-stead of «special electrometallurgy». Naturally, the terminology will be valid only during some period of time. In any case the analysis of the state-of-the-art and prospects of special electrometallurgy will be not comprehensive without estimation of tendencies in the development of the ferrous metallurgy.

Let us try to analyze some tendencies and prospects in the development of the big metallurgy, and then in special electrometallurgy, its most important sub-branch. This is especially important, because steel remains a major structural material in the modern world, while for Ukraine and Russia the ferrous metallurgy (and special electrometallurgy) is and will be the key branch of economy for the nearest years.

Over recent 40−50 years the radical changes were observed in the ferrous metallurgy both in the creation of the quite new technologies and materials, and also in the updating of the traditional ones. It seems, that during this period a basic oxygen furnace (BOF) production of steel, its ladle treatment and continuous casting were really epochal for the ferrous metallurgy. There were these three key technological processes that defined the technical and economical status of the modern metallurgical production (even direct reduction of iron today has a less importance).

It seemed by the end of the 1980s and beginning of the 1990s of the last century that the epoch of rapid changes had finished, and the period of accumulation, gradual updating has come in the metallurgy. However, it was exactly that period when a new stage of qualitative changes began. Unfortunately, our metallurgists know little about the name of a man who personified that time. His name was Ken Iverson. It was the man, who, being the head of US Company «Nucor Steel», realizing the production of steel at a conventional mini-factory, decided first in the world to organize all the production of the company on the basis of a continuous casting of thin slabs and their subsequent direct rolling for the sheet. The quite real idea to make section of a continuously-cast billet close

---

[*]This article was presented as a paper at the International Scientific-Technical Conference on Special Metallurgy: Yesterday, Today, Tomorrow, Oct. 8−9, 2002, Kyiv, Ukraine.
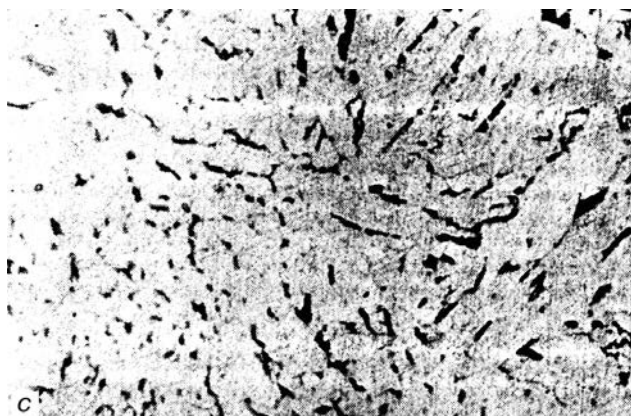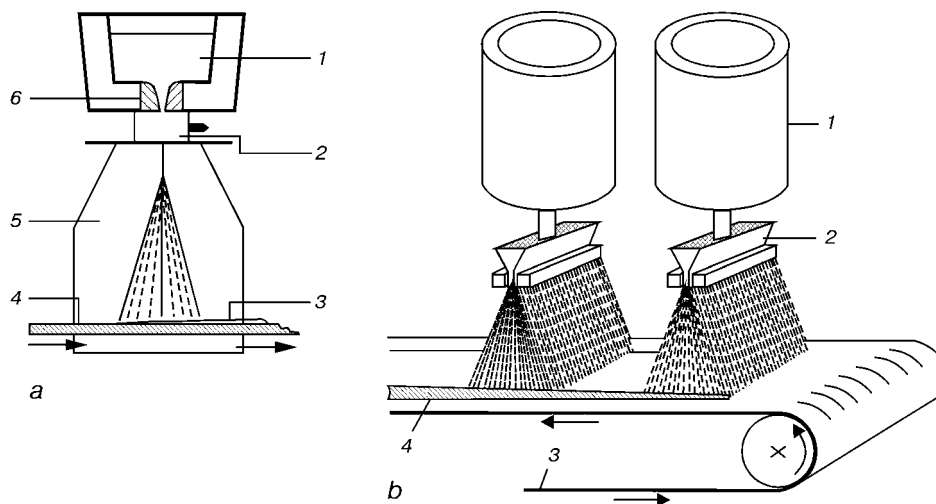
Diagrams of spraying processes: a — O'Sprey (1 — molten metal; 2 — transition piece; 3 — strip; 4 — substrate; 5 — chamber with inert gas; 6 — round nozzle); b — LDC (1 — molten metal; 2 — longitudinal nozzle; 3 — «continuous» substrate; 4 — strip); c — microstructure of strip of steel 08kp (rimmed) produced by spraying (×100)

to that of a rolled product, and, moreover, to combine casting and rolling into a single and continuous line, a single unit, sometimes called today casting-rolling [1], attracted metallurgists long ago. It is also natural that by the moment of progress of «Nucor Steel», i.e. 15 years ago, there were many different, as now called «pilot» projects of a continuous casting of thin slabs in the world. The problem was to make a decision and Ken Iverson did not afraid to do this. And at present more than 30 million tons of steel in the world are produced using this method. The Company «Nucor Steel» itself has transformed from a mini-factory to the largest steel manufacturer in the USA. Ken Iverson described his life as a head of the most modern and successful metallurgical enterprise in book «Talk Plain» [2]. The revolutionary decisions of this person, died in April this year, are similar to those which are well-known in our country. The question is about such a non-ordinary person as Nikita S. Khrushchev and his decision to buy license on BOF melting for Novolipetsk Metallurgical Works.

It were these daring decisions of that time that led to the appearance of the first in the world plant with 100 % continuous casting of steel, first of all, of BOF melting. There is no need to prove that in a full conformity to laws of dialectics the ferrous metallurgy at present is at the stage of quantitative changes, and this means, that the next stage of a jumpy transition of quantity into quality is waiting for us ahead. Perhaps, the only chance of metallurgists of our country is to perform a qualitative jump now, but not only to repeat the already passed way and to try to overtake the advanced metallurgical companies at the expense of a cheap labour and purchase of the most advanced at present technologies and equipment, but already used by somebody and somewhere. Only combination of a reasonable risk with the use of the newest research and technological developments will allow both Ukraine and Russia to return to the rank of the leading metallurgical countries.

Example with BOF processing and continuous casting has already become classical for the metallurgists of the former USSR. However, all this was in the past. What really new can be recommended today? Have we now the pioneering developments, similar to evaporating cooling of blast furnaces or ESR, whose licenses were bought almost by all the industrialized countries? We think, they exist. Each leader of our metallurgical industry should, on the basis of the world scientific achievements, carry out own search and take solutions and then the really unique and new technologies and equipment will appear at the metallurgical plants of our country. It is necessary to remember that the scientists in the field of materials science were always mighty in the former USSR and they remain as such today.

Here, we would like to dwell on two potential capabilities, which, in our opinion, have not yet found a deserving understanding. The question is about such traditional materials for metallurgists as a rimmed steel and bimetal.

More than 10 years ago it was shown [3] that it is possible to form the 10–20 mm thick continuous strip of rimmed steel and to convey it to the rolling mill using such processes of molten metal spraying as O'Sprey and/or Liquid Dynamic Compaction (LDC) (Figure). There are all the grounds to suppose that the steel quality due to the highest rate of so-

lidification will be acceptable for its use equally with a killed steel.

Advantages of bimetal products are known long ago. A lot of work in this field was done at our Institute. Even today the bimetal sheet of the highest quality is produced using electroslag remelting and cladding. Now, the first symptoms appeared that in the nearest time the bimetal rolled metal in the form of various shapes of building assortment in particular, including reinforced steel, will be wider and wider used in industry. The Table presents data of Company «Stelax» about the corrosion resistance of a traditional reinforcement, made of stainless steel and bimetal, named Nuovinox, and gives the comparison of cost of reinforcement of different types. These data are very impressive and do not need additional comments. In addition, during recently the bimetal products (not only reinforcement) of this Company became to be used wider in repair and construction of new bridges and introduced into appropriate standard documents in the USA. These products can be produced using the varieties of ESR with a liquid metal, without consumable electrodes, which were developed at our Institute over the recent years [4].

At present many new structural materials are appeared to satisfy the needs of aircraft, space and other industries, as was accepted to say for «critical applications». However, the example of Nuovinox proves that structural steels will also become in the nearest future different and metallurgists should be ready today to the soon changes in the market even of traditional kinds of rolled metal.

Challenge of time greatly influences also the special electrometallurgy. We suppose that the prospects of the special electrometallurgy are observed today in the production of superalloys, titanium and its alloys, as well as of intermetallics for both power and aircraft gas turbine construction. It is expected, that the next qualitative jump both in technologies and materials will begin in the field of a special electrometallurgy.

All these various technological processes are common now in the fact that they should be carried out, and in some cases they are already carried out, only on the basis of a careful mathematical modelling of metal structure required by customers, but not of a simple design of a profile and depth of two-phase zone in solidification of ingots. The experience of application of this kind of models in melting superalloys is positive. And today the development of technology of VAR and ESR of alloys of Inconel types is based on mathematical modelling without full-scale expensive melts. It is evident, that to obtain these results a perfect system of control of technological processes is required to guarantee the constancy of conditions of metal solidification during all the melting. It is possible to say with a confidence that the key trend in the special electrometallurgy in the nearest years will be development of the system of monitoring and control of melting alloys of different types on the basis of study of specifics of their crystallization and

Material of reinforcement section	Mean service life before first repair, years	Relative cost of reinforcement section
Carbon steel	8–20	1
Carbon steel coated by epoxy resin	13–25	1.5
Bimetal: carbon steel + stainless steel	75	3
Stainless steel	75	6.5

structure formation. In other words, it would be necessary to examine the peculiarities of structure formation of each type of alloys, to construct an appropriate mathematical model and to perform melting purposefully, presetting both the producing matrix, and also either form and distribution of second phases of the given alloy.

We see the future of the special electrometallurgy in realization of unique potentialities to influence purposefully on the metal structure. It is especially important in connection with a rapid growth of production and application of nanocrystalline materials. Here, it is important to take into account that any alloy can be in principle considered as a composite material and the metallurgists of a classical class should prepare themselves to such interpretation of structural metallic materials of the future. Today we can guarantee the optimum combination of service properties only for a rather limited number of steels and alloys because of the absence of technological capabilities of a purposeful control of the structure. In the number of these rare exclusions, there are metals, for example, which are passing the heat-mechanical treatment, including the controllable rolling and multilayer metals, including also bimetals. In its time when working with multilayer steels the associates of the PWI suggested to consider them as steels with preset anisotropy of structure [5]. Today it is necessary to widen this approach and consider alloys as materials with a preset anisotropy of the properties.

It should be noted in conclusion, that even most cautious and most optimistic predictions are often refuted by the reality. Nevertheless, we shall take a risk to suppose that the special electrometallurgy will have a good future. And the main problems, which are to be solved, will be related to materials for power and aerospace engineering. And the solution of these problems will be on the way of an integrated application of different technologies as it is done today in production of superalloys by a successive vacuum-induction melting, ESR and final VAR.

1. Dubina, O.V., Ostapenko, A.L., Nikitina, L.A. et al. (2002) Technology and equipment, problems and prospects of continuous hot rolling in wide-strip mills. *Bull. Chermetinform.*, **5**, 10–31.
2. Iverson, K. (1997) *Talk Plain. Lessons from business maverick*. AISE.
3. Paton, B.E., Medovar, B.I., Medovar, L.B. et al. (1991) On liquid-dynamic compaction of steel. *Doklady AN SSSR, Tekhnich. Fizika*, **4**, 730–732.
4. Tsykulenko, K.A. (2002) Electroslag cladding with liquid metal. In: *Proc. of Int. Conf. on Special Metallurgy: Yesterday, Today, Tomorrow*. Kyiv: Politekhnika.
5. Paton, B.E., Medovar, B.I., Tsykulenko, A.K. et al. (1984) *Multilayer steel in welded structures*. Kyiv: Naukova Dumka.

INVESTIGATION OF INTERPHASE INTERACTION OF FERROTITANIUM WITH SILICON CARBIDE IN POWDER MIXTURES USED FOR THERMAL SPRAY COATING

G.M. GRIGORENKO, A.L. BORISOVA, Yu.S. BORISOV, L.I. ADEEVA, L.K. DOROSHENKO and **V.L. RUPCHEV**

The E.O. Paton Electric Welding Institute, NASU, Kyiv, Ukraine

Exothermal interaction in FeTi−SiC system was investigated. Maximum exothermal effect was achieved is use of 79 wt.% FeTi + 21 wt.% SiC mixture with the formation of TiC, $Ti_5Si_{3-x}C_x$, Fe_3Si, Fe_5Si_3 as products of interaction. The powder mixture of this composition is most challenging for producing composite powders and spraying of thermal coatings with a high wear and corrosion resistance.

Key words: *thermodynamic calculations of equilibriums, exothermal effect, differential thermal analysis, microstructure, phases of Fe−Ti−Si−C system*

In the present work the interaction of ferrotitanium with silicon carbide using a method of differential thermal analysis (DTA) was studied to select the composition of a composite powder of Fe−Ti−Si−C system, optimum for producing wear-resistant coatings by thermal spraying. In earlier works [1−3] the interaction in composite powders Ti−SiC and properties of coatings produced from them by the method of a plasma spraying were investigated. Here, the prospects of use of the developed coatings for protection of friction units of fuel equipment, machine and equipment parts from wear are shown. To reduce the cost of initial materials for coating deposition and also the level of internal stresses at the interface of coating with a metal base (steel), titanium was replaced by ferrotitanium.

The investigation of interaction of ferrotitanium with silicon carbide was made using methods of thermodynamic, differential thermal, metallographic, microdurometric and X-ray diffraction phase analysis.

Evaluation of feasibility of proceeding the simplest reactions of titanium and iron with silicon carbide was made on the basis of thermodynamic calculations of changes in values of isobaric-isothermal potential ΔZ (Gibbs energy). Calculations were made using known methods [4, 5] and most valid initial thermodynamic data [6−9]. It was assumed here that the reactions are proceeding with participating of insoluble phases.

Adiabatic increase in temperature as a result of proceeding reaction can be presented in the form

$$\Delta t_{ad} = \frac{Q_{ex}}{C_p},$$

where Q_{ex} is the thermal effect of interaction; C_p is the heat capacity of reaction products.

In absence of values C_p its averaged value was used in some definite cases for simple substances and compounds which was equal to 33.5 kJ/(kg-atom·deg) from data of Kelley [4]. Results of calculations are given in Figures 1 and 2 and Tables 1 and 2.

In interaction of silicon carbide with titanium the reactions of formation of mixture of phases: titanium carbide with titanium silicides (Figure 1, curves 5−7) are most probable thermodynamically. Moreover, in transition from Ti5Si3 to TiSi and then to TiSi2 the

Table 1. Thermal activity of reactions of silicon carbide with titanium

No.	Reactions	Content of SiC		Value of heat effect			Δt_{ad}, °C
		wt.%	vol.%	kJ/(g·mol) of SiC	kJ/kg of mixture	kJ/cm³ of mixture	
1	SiC + Ti = TiC + Si	46	54	111.70	1269	4.84	1110
2	SiC + 5/3Ti = 1/3Ti5Si3 + C	33	41	121.96	1016	4.04	992
3	SiC + Ti = TiSi + C	46	54	57.80	65	2.51	575
4	SiC + 1/2Ti = 1/2TiSi2 + C	62.5	70	−4.75	−74	−0.27	−56
5	SiC + 8/3Ti = TiC + 1/3Ti5Si3	24	30	305.64	1821	7.49	1954
6	SiC + 2Ti = TiC + TiSi	30	37	241.48	1795	7.22	1802
7	SiC + 3/2Ti = TiC + 1/2TiSi2	36	44	178.94	1598	6.30	1526

Table 2. Thermal activity of reactions of silicon carbide with iron

No	Reactions	Content of SiC		Value of heat effect			Δt_{ad}, °C
		wt.%	vol.%	kJ/(g·mol) of SiC	kJ/kg of mixture	kJ/cm³ of mixture	
1	$SiC + 3Fe = Fe_3Si + C$	19	37	21.96	106	0.65	131
2	$SiC + 5/3Fe = 1/3Fe_5Si_3 + C$	30	51	9.67	73	0.40	79
3	$SiC + Fe = FeSi + C$	42	64	4.67	49	0.24	47
4	$SiC + 1/2Fe = 1/2FeSi_2 + C$	59	78	−31.25	−459	−1.95	−37
5	$SiC + 3Fe = Fe_3C + Si$	19	37	−46.8	−225	−1.39	−279
6	$SiC + 6Fe = Fe_3C + Fe_3Si$	11	23	−3.14	−84	−0.06	−12
7	$SiC + 14/3Fe = Fe_3C + 1/3Fe_5Si_3$	13	27	−15.43	−51	−0.34	−69
8	$SiC + 4Fe = Fe_3C + FeSi$	15	30	−20.43	−77	−0.5	−102
9	$SiC + 3.5Fe = Fe_3C + 1/2FeSi_2$	17	33	−56.35	−239	−1.51	−31

probability of reaction is diminished. Reaction of formation of lower titanium silicide Ti_5Si_3 with precipitation of a free carbon is impossible thermodynamically (curve 4), the other reactions occupy the intermediate position. Exothermicity of reactions considered is sufficiently high, the highest adiabatic peak of temperature reaches almost 2000 °C (Table 1).

In interaction of silicon carbide with iron the reactions of formation of silicides with precipitation of a free carbon (Figure 2, curves 1–3) are most probable, here the degree of their probability is increased in the row FeSi→Fe_5Si_3→Fe_3Si. Reactions of formation of the same silicides in mixture with Fe_3C are possible at temperatures above 200, 400 and 700 °C for silicides Fe_3Si, Fe_5Si_3, FeSi, respectively (curves 6–8). Reactions of $FeSi_2$ formation with precipitation of a free carbon, Fe_3C with precipitation of a free silicon and mixtures $FeSi_2$ and Fe_3C (curves 4, 5, 9) are impossible within the entire temperature interval (up to 1500 °C). Adiabatic peak of temperature does not exceed 130 °C (Table 2).

Thus, in interaction of ferrotitanium with silicon carbide the formation of mixture of phases should be

expected: titanium carbide, titanium silicides (first of all Ti_5Si_3) and iron silicides (probability of Fe_3Si, Fe_5Si_3 and FeSi formation is differed negligibly).

Due to the absence of initial thermodynamic data the feasibility of formation of ternary or more complex compounds, as well as solid solutions was not considered in calculations. Nevertheless, the existence of two ternary compounds is known in the Ti–Si–C system [10]: Fe_3SiC_2 and $Ti_5Si_{3-x}C_x$ which were revealed earlier by us in products of interaction of powder mixtures of titanium with silicon carbide [1].

For experimental investigation of ferrotitanium interaction with silicon carbide the compositions of mixtures were selected, which were characterized by the highest degree of exothermal activity, namely Ti + 24 wt.% SiC (Table 1, reaction No.5), Fe + 19 wt.% SiC (Table 2, reaction No.1). Composition of mixtures with ferrotitanium which contains 50 at.% Fe (54 wt.%) and 50 at.% Ti (46 wt.%) should be as follows: 79 wt.% FeTi + 21 wt.% SiC.

As initial material the powders of ferrotitanium with 40–100 μm size of particles, silicon carbide of two fractions (80–160 μm and < 3 μm) produced by the method of grinding were used for investigations. Powders of pure iron and titanium had < 5 μm size
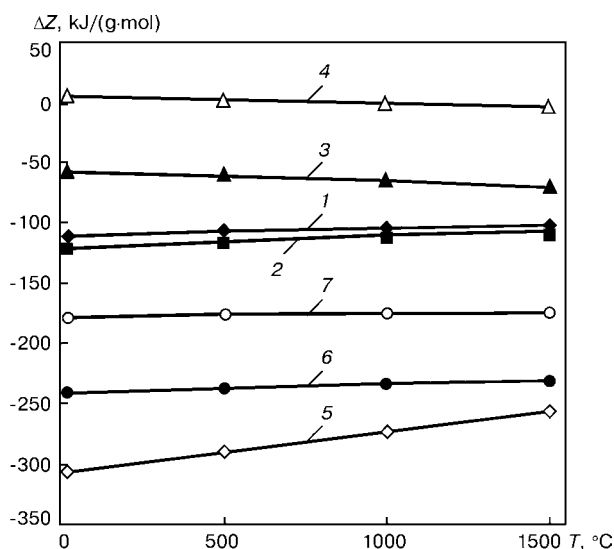
Figure 1. Temperature relationship in changing Gibbs energy during reaction of silicon carbide with titanium (figures on curves correspond to numbers of reactions in Table 1)
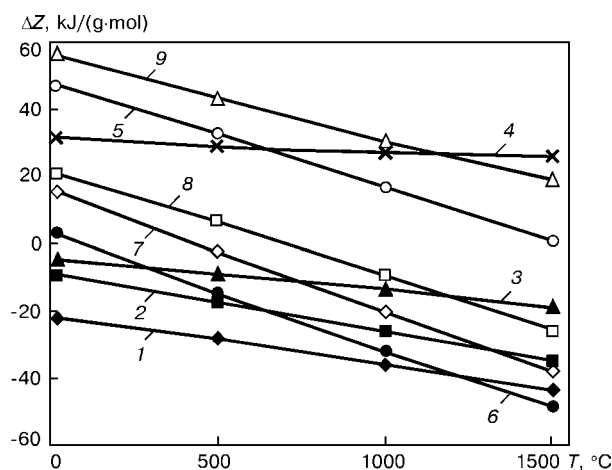
Figure 2. Temperature relationship in changing Gibbs energy during reaction of silicon carbide with iron (figures on curves correspond to numbers of reactions in Table 2)

ΔT, °C
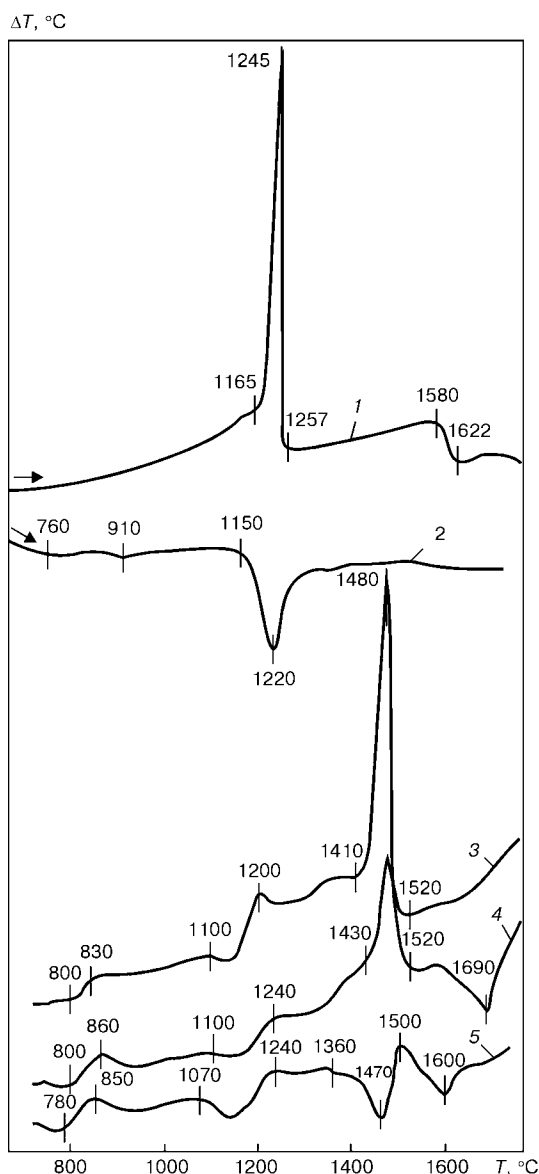
Figure 3. Differential thermal curves of heating powder mixtures of composition, wt.%: *1* — 76Ti + 24SiC; *2* — 81Fe + 19SiC; *3* — 79FeTi + 21SiC; *4* — 86FeTi + 14SiC; *5* — 91FeTi + 9SiC

of particles. X-ray diffraction phase analysis showed that only powder of ferrotitanium contains, except phase FeTi, a small amount of Fe_2Ti, γ-FeTiO and TiC_{1-x}. The rest powders do not contain impurities, the silicon carbide has a structure with a hexagonal lattice.

Samples for DTA were prepared from initial powders by careful mixing in HSM type mixer of «Herzog» Company and subsequent pressing at 3 t/cm^2

pressure. DTA was made in unit VDTA-8M in a static medium of helium at 80 K/min rate of cooling.

Analysis of differential thermal curves of heating powder mixtures (Figure 3) showed that DTA curve *3* for FeTi–SiC has a number of common features with curves *1* and *2* for Ti–SiC and Fe–SiC, respectively. Thus, the endothermal effect is observed on curves *2* and *3* at temperature above 1100 °C, while on curves *1* and *3* the sharp peak of exothermal effect at temperatures 1245 and 1480 °C, respectively, is observed.

The X-ray diffraction phase analysis of samples (Table 3) showed that interaction of powders Fe + SiC in mixture is proceeding mainly with the formation of silicide phases of iron (Fe_5Si_3, Fe_3Si and FeSi). Endothermal peak at temperatures 1150–1220 °C is due to the appearance of the liquid phase, i.e. eutectic Fe_3Si–Fe_5Si_3 (T_{melt} = 1250 °C [11]).

In FeTi–SiC system the interaction is started, probably, with the formation of iron silicides. The appearance of liquid phase (eutectic), promoting the acceleration of transfer of reagents to the reaction zone, leads to the transition of the first (slow) stage into the stage of active interaction with an abrupt rise of temperature as a result of reaction of silicon carbide with titanium contained in the ferrotitanium composition.

The presence of iron in mixture FeTi–SiC and formation of iron silicides at the first stage, unlike Ti–SiC, leads to shifting the temperature interval of active interaction to the region of the higher temperatures. Comparison of phase composition of ingots produced at DTA and phases expected on the basis of thermodynamic estimates showed that products of reactions contain additionally (though in a small amount) the ternary compounds and solid solutions (Table 3). In other respects the results of experimental investigation confirm the data of the thermodynamical analysis. The main products of interaction of FeTi with SiC are the iron and titanium silicides, and also titanium carbide. The latter, having a wide region of homogeneity, binds carbon precipitating according to reaction

$$m\text{Fe} + n\text{SiC} = \text{Fe}_m\text{Si}_n + n\text{C}.$$
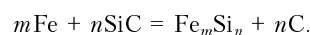
In comparison of microstructure and phase composition of ingots, produced from mixtures of ferrotitanium with silicon carbide of different dispersity (80–160 μm and < 3 μm), it was outlined that in the first case the reaction is not proceeding to the end (lines SiC, FeTi and Fe_2Ti were revealed on radio-

Table 3. Characteristic of most exothermal mixtures of reaction products

Mixture composition, wt.%	Phase composition		Microhardness, GPa
	calculated	experimental	
79FeTi + 21SiC	TiC, Ti$_5$Si$_3$, Fe$_3$Si, FeSi, Fe$_5$Si$_3$	TiC$_{1-x}$, Ti$_5$Si$_{3-x}$C$_x$, Fe$_3$Si, FeSi, Fe$_5$Si$_3$	15.3–20.6 (carbide inclusions) 9.46–11.59 (silicide matrix)
81Fe + 19SiC	Fe$_3$Si, FeSi, Fe$_5$Si$_3$, C	Fe$_3$Si, FeSi, Fe$_5$Si$_3$, Fe$_8$Si$_2$C, Fe–C solid solution	4.0–8.0
76Ti + 24SiC	TiC, Ti$_5$Si$_3$,	TiC$_{1-x}$, Ti$_5$Si$_{3-x}$C$_x$	18.1–23.3 (carbide inclusions) 12.5–12.7 (silicide matrix)
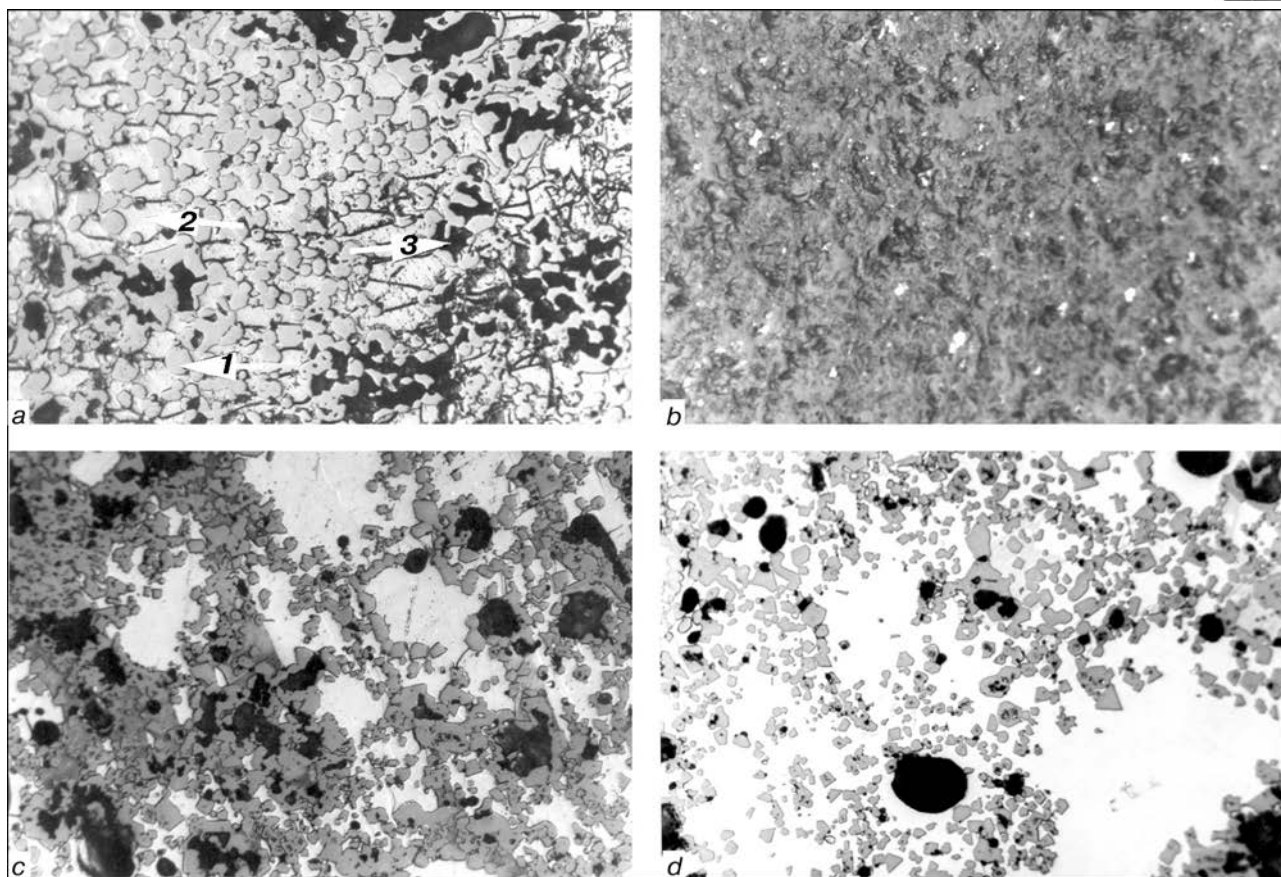
Figure 4. Microstructure of products of interaction of ferrotitanium with silicon carbide (not etched): *a, b* — 21 wt.% SiC (*1* — titanium carbides; *2* — silicides of titanium and iron; *3* — silicon carbides) (×650); *c* — 14 wt.% SiC; *d* — 9 wt.% SiC (×400)

grams) and there are pores in the ingot structure (Figure 4, *a*). In the second case the structure is more homogeneous, fine-dispersed, pores on microsections are not seen even at much higher magnification (Figure 4, *b*). Structure of similar type is most preferable for corrosion-resistant coatings operating for wear.

To check the effect of silicon carbide in mixture with ferrotitanium on its exothermicity, the experiments were performed with 14 and 9 wt.% SiC (Figure 3, curves *4* and *5*). Results show the reduction of thermal activity of mixture with a decrease of silicon carbide amount in it. Here, the ingot structure becomes less homogeneous (Figure 4, *c, d*), microhardness of matrix is decreased (for FeTi + 9 wt.% SiC — up to 7.2 GPa), that is associated with the presence of a non-reacted ferrotitanium in it. With SiC increase in mixture as compared with optimum content (more than 21 wt.%) the large amount of residual SiC is preserved in the ingot, i.e. the reaction is proceeding up to the end, resulting in decrease in ingot strength.

Thus, the interaction of FeTi with SiC in powder mixtures has an exothermal nature. Titanium replacement by ferrotitanium leads to some decrease in exothermicity of the process of interaction with SiC and increase in temperature of beginning the active interaction approximately by 250 °C that is caused by the formation of iron silicides and their fusible eutectics. Based on experimental data corresponding to theoretical calculations the maximum exothermal

effect is attained in use of mixtures 79 wt.% FeTi + 21 wt.% SiC with the formation of TiC, $Ti_5Si_{3-x}C_x$, Fe_3Si, Fe_5Si_3 as interaction products, whose microhardness is 15.3–20.6 and 9.46–11.59 GPa for carbide and silicide matrix, respectively. This combination of structure components, i.e. hard carbide inclusions in more soft and plastic silicide matrix, are most optimum for thermal coatings with a high wear and corrosion resistance.

1. Borisova, A.L., Borisov, Yu.S., Polyanin, B.A. et al. (1985) Interaction of Ti–SiC in composite powders and properties of sprayed coatings. *Poroshkovaya Metallurgiya*, **10**, 92–96.
2. Borisova, A.L., Shvedova, L.K., Marshchenyuk, I.S. (1985) Interface interaction in composite powders of metal–non-metallic refractory compound. In: *Adhesion of melts and brazing of metals*, Issue 15, 59–64.
3. Borisov, Yu.S., Borisova, A.L., Adeeva, L.I. et al. (1995) Composite plasma coatings of Ti–Si–C system. *Problemy Spets. Elektrometallurgii*, **3**, 62–71.
4. Krestovnikov, A.N., Vigdorovich, V.N. (1961) *Chemical thermodynamics*. Moscow: Metallurgizdat.
5. Kubashevsky, O., Evans, E. (1954) *Thermochemistry in metallurgy*. Moscow: Inostr. Literatura.
6. (1986) *Properties, production and application of refractory compounds*. Refer. Book. Ed. by T.Ya. Kosolapova. Moscow: Metallurgiya.
7. Wix, C.E., Block, F.E. (1965) *Thermodynamical properties of 65 elements, their oxides, halogens*. Moscow: Metallurgiya.
8. Vojtovich, R.F. (1971) *Refractory compounds. Thermodynamical characteristics*. Refer. Book. Kyiv: Naukova Dumka.
9. Veryatin, U.D., Mashirev, V.P., Ryabtsev, N.G. et al. (1965) *Thermodynamical properties of inorganic substances*. Refer. Book. Moscow: Atomizdat.
10. Nickl, J., Schwitzer, K., Luxenberg, P. (1972) *Gasphasenabscheidung im system Ti–Si–C. J. Less Common Metals*, **3**, 335–353.
11. Hansen, M., Anderko, K. (1962) *Structures of binary alloys*. Moscow: Metallurgizdat.

INVESTIGATION OF PHASE TRANSFORMATIONS IN COMMERCIAL FERROSILICIUM USING THE METHOD OF SYNCHRONOUS THERMAL ANALYSIS

M.M. GASIK, V.L. ZUBOV and **M.I. GASIK**

National Metallurgical Academy of Ukraine, Dnepropetrovsk, Ukraine

Results of experimental study of phase transformations in ferrosilicium of FS45, FS65 and FS70 grades by a synchronous thermal analysis using a differential scanning calorimetry (DSC) and thermogravimetry are considered. Thermal effects occurring in heating and cooling as a result of phase transformations are estimated quantitatively. The change in mass of samples in the process of heating and cooling, and also the heat capacity of ferrosilicium within the temperature 20−1350 °C interval are determined. Comparative analysis of temperature transformations in ferrosilicium of different grades by position of peaks of DSC curves was made.

Key words: *high-silicon ferrosilicium, Fe−Si state diagram, phase transformations, synchronous thermal analysis (differential scanning calorimetry, thermogravimetry), thermal effects of transformations*

Electrothermal ferrosilicium covers by its chemical composition a wide concentration region of state diagram of Fe−Si system, namely from 19 up to ≥ 92 % Si (GOST 1415−93) [1, 2]. In this connection the selection of ferrosilicium composition, technology of casting and also its application in steel-making industry in deoxidizing and alloying of steels and alloys of a different functional purpose is defined mainly by the level of knowledge and availability of valid thermodynamic data about the properties of ferrosilicium of each grade.

Analysis of literature data shows that the stable state diagram of Fe−Si system has been studied comprehensively owing to fundamental investigations made during the recent decades at the end of the last century, though there are some problems, such as compositions and types of crystalline structures of compounds, temperatures of phase transformations (first of all lebeauite) which continue to remain open to discussions [3, 4].

Electrothermal ferrosilicium of industrial melting contains a number of impurity elements among which aluminium, calcium, manganese, chromium, titanium, phosphorus, sulphur and carbon are regulated by GOST 1415−95. The presence of these elements has a definite effect on phase transformations in ferrosilicium during formation of structure, developing of liquation phenomena, precipitation of excessive phases in ingots and also intensive their susceptibility to the phenomenon of a self-crumbling in a humid atmosphere with a formation of poison gases of phosphine and arsine [5, 6].

Production of ferrosilicium has an export-oriented nature, that defines its grade composition. These are mainly FS45, FS65 and FS70 (FS75 rarely). In this connection the phase transformations in ferrosilicium

of « elite» grades, competitive at national and international markets of ferrosilicium products were investigated in the present work. Samples of commercial ferrosilicium of three grades of present-day production were used (Table 1).

Phase transformations in heating (cooling) of ferrosilicium samples were examined using a method of a synchronous thermal analysis representing a combination of methods of gravimetry and DSC. Principle of DSC consists in a dynamic changing of a heat flow, directed to the ferrosilicium sample examined. This change is necessary for compensation in the difference of temperatures between the sample and reference (sapphire). As compared with equipment used traditionally for differential thermal analysis, the equipment for temperature measuring in DSC has a special design of a measuring part and is characterized by a higher sensitivity.

The aim of the present work is to establish temperatures and enthalpies of phase transformations (reactions) in heating (cooling) of ferrosilicium samples by chemical composition referring to a concentration region FeSi−Si of state diagram of Fe−Si system (Figure 1).

The investigations were performed in unit Jupiter STA 449C which makes it possible to perform the synchronous thermal analysis with a sensitivity by mass up to 0.1 μg and by enthalpy up to 2 %. Samples of 0.3−0.4 g were heated in atmosphere of a pure

Table 1. Chemical composition of samples of commercial ferrosilicium (GOST 1415−93)

Ferrosilicium grade	Content, wt.%							
	Si	Al	Mn	Cr	Ti	Cu	P	S
FS45	45.5	0.4	0.3	0.4	0.1	0.09	0.03	0.01
FS65	64.0	0.6	0.2	0.2	0.2	0.09	0.03	0.01
FS70	72.2	2.3	0.2	0.2	0.2	0.05	0.02	0.01
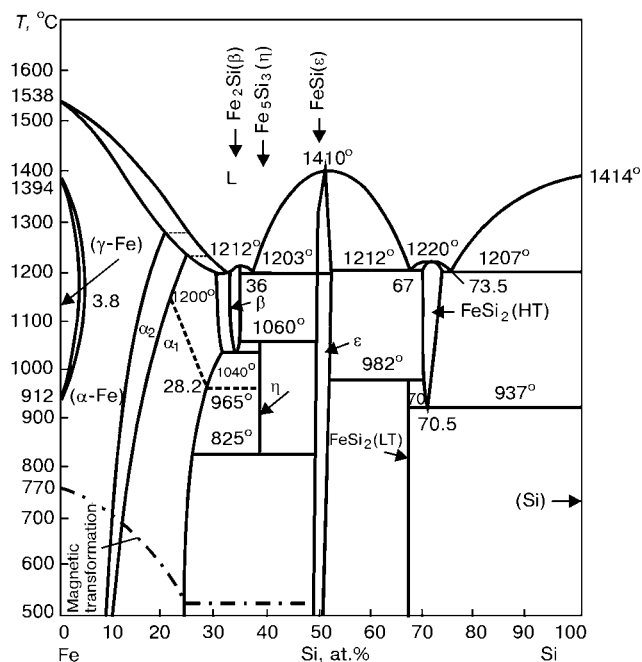
Figure 1. State diagram of binary Fe−Si system

Table 2. Theoretical values of specific heat capacity, $J/(g\cdot K)$, of silicon and silicide phases in independent system FeSi−Si

Phase	$C_p = A + B \cdot 10^{-3} T + C T^{-2} + D \cdot 10^{-9} T^2$				
	A	B	C	D	T, K
Si	0.81264	0.13736	−12600	−	298−1685
FeSi$_{2.43}$	0.60689	−	−	−	298−398
FeSi$_{2.33}$	0.58282	0.2783	−6799.63	−	298−900
β-FeSi$_2$	0.4946	0.2606	44.635	−	298−900
FeSi	0.4553	0.26714	319.3	−2.44	298−1683

N o t e. Database HSC 4.01, Outokumpu Research, Finland; TAPP 3.0, ESM Inc., USA.

$$C_p = \frac{m_{std}}{m_s} \frac{DSC_s - DSC_{base}}{DSC_{std} - DSC_{base}} C_{p_{std}},$$

where indices «*s*», «*std*», «*base*» are the sample, standard and base line, respectively; *DSC* is the signal.

argon in alundum calibrated crucibles at the rate of 20 °C/min up to 1350 °C, 30 min holding and cooling at 5 °C/min rate with recording of change in mass and temperature. A sapphire disc with a known heat capacity was used as a reference sample. Experimental data and correlation curve of a specific heat capacity of sapphire depending on temperature obtained during calibration of the instrument are given in Figure 2. Theoretical values of heat capacity of phases of independent system FeSi−Si are presented in Table 2.

The heat capacity of ferrosilicium samples is determined by formula

$$C_p = \frac{dH}{dT} \Big/ m\left(T(\tau)\right),$$

where *dH* is the enthalpy change; *T* is the temperature; *m* is the sample mass which can depend on time τ and temperature. Therefore, the specific heat capacity can be presented in accordance with the DSC method by the expression

Below, the results of our experiments and their analysis are given. Typical curves of DSC and thermogravimetry of thermal analysis of ferrosilicium of FS45 grade are shown in Figure 3. Hatched line characterizes the rise of temperature of alloy sample in an alundum crucible with time at a preset constant rate (20 °C/min), isothermal holding during 30 min and cooling of sample with a crucible at 5 °C/min rate. The mass of ferrosilicium sample is increased only in the region of heating and holding at the expense, probably, of alloy oxidation, while in cooling it remains almost constant within the interval of temperatures from 1200 °C and lower that is proved by a horizontal region on curve *m*.

Figure 4, *a, b* presents the DSC comparative curves of all the alloys in heating and cooling, respectively. The change in mass of ferrosilicium samples in experiments was negligible, i.e. to 0.5 %. By comparing most clear peaks on DSC curves (Figure 4, *a*) of thermal analysis of ferrosilicium of three grades with a stable state diagram of Fe−Si system, it was shown that the position of these peaks, in spite of high rate of heating samples (20 °C/min) has a good correlation with temperature phase transformations in FeSi−Si independent system.

At the same time, in cooling samples of alloys at a lower rate (5 °C/min) as compared with that of heating the effect of overcooling (by 10−40 °C) is

Figure 2. Dependence of specific heat capacity of sapphire (α-Al$_2$O$_3$) on temperature (signs of correlation curve − experimental data)
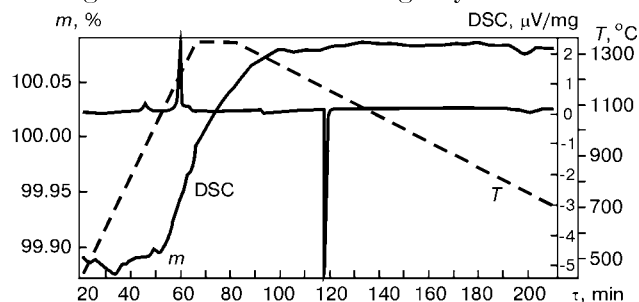
Figure 3. Typical curves of differential scanning calorimetry and thermogravimetry
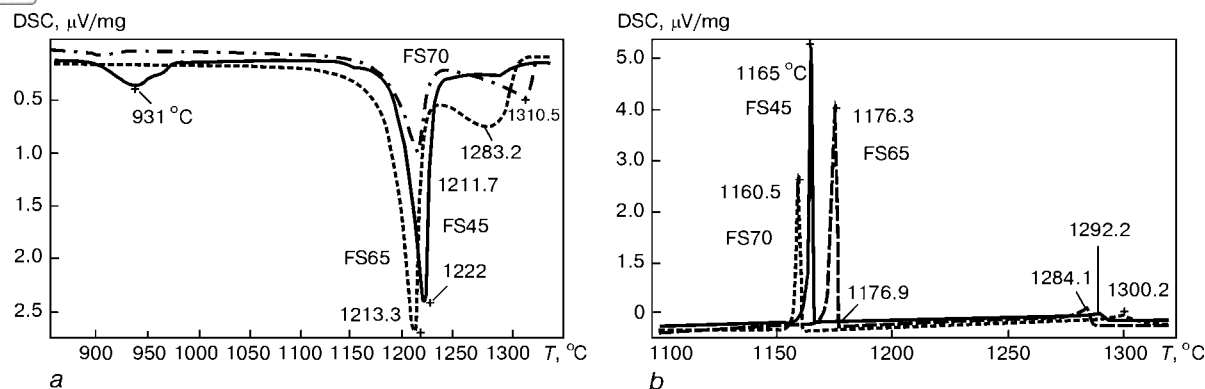
Figure 4. Comparative DSC curves of alloys FS45, FS65, FS70 in heating (*a*) and cooling (*b*)

manifested that can be caused by the effect of impurity elements in ferrosilicium on the temperatures of eutectics, as the liquidus temperature is coincided almost with appropriate temperatures of melting alloys from the data of stable state diagram of Fe–Si system (Figure 4, *b*).

Identification of peaks on DSC curve of ferrosilicium of FS45 grade enables us to make a conclusion that the alloy undergoes the eutectic transformation in heating up to 1223 °C (cooling 1166 °C) and liquidus transformation at 1289–1304 °C (cooling 1288 °C). Ferrosilicium FS65 undergoes eutectic transformation in heating up to 1213 °C (cooling 1176 °C). At further increase of temperature this alloy undergoes liquidus transformation at 1283 °C (cooling 1284 °C). Almost complete coincidence of liquidus in heating and cooling of samples of ferrosilicium of FS45 and FS65 grades was stipulated by a very low temperature interval of solidus–liquidus transformation, though liquidus of commercial ferrosilicium of FS65 grade is by about 50 °C higher than the temperature of melting of $FeSi_{2.3}$ silicide. Temperatures of phase transformations from data of identified DSC peaks for ferrosilicium of FS45, FS65 and FS70 grades are given in Table 3.

In accordance with an independent state diagram of FeSi–Si system the eutectic-1 represents $FeSi_{2.3}$ (lebeauite) + FeSi, eutectic-2 — Si + $FeSi_{2.3}$, and

liquiduses 1 and 2 are the temperatures of transition from two-phase regions (solid–liquid) into a liquid state.

On DSC curves of alloys FS45 and FS70 some peaks are revealed which could not be identified in spite of their repetition at successive heating (cooling) of samples. These peaks are due to the transformations in alloys in a solid state, though one peak 1255 °C is revealed in heating sample of alloy FS45 in a two-phase temperature region.

The assuming reactions for interpretation of non-identified peaks on DSC curves for alloys FS45 and FS70 are given in Table 4.

Thermokinetic analysis of melting (solidification) of ferrosilicium. The thermokinetic analysis of melting ferrosilicium has a theoretical and practical importance and, first of all, as was above-mentioned, in deoxidizing and alloying of steel. It was not managed to find results in literature of a similar thermal analysis of eutectic reactions existing in melting (solidification) of ferrosilicium of FS45, FS65 and FS70 grades. To compensate this lack of data the experimental DSC curves in the present work were processed, after a necessary correction (zero line of instrument and thermal resistance of alloy sample), using a method of a non-linear regression with analysis of possible types of reactions (of first, second and higher

Table 3. Comparison of temperatures of DSC peaks of different alloys in heating (above line) and cooling (under line)

Possible transformation	Temperature of phase transformation, °C			
	FS45	FS65	FS70	From state diagram (Figure 1)
Eutectic-1	1223 1166	–	–	1212
Eutectic-2	–	1213 1176	1212 1160	1207
Liquidus-1	1289–1304 1288	–	–	1300
Liquidus-2	–	1283 1284	1310 1300	1285 (65 %), 1310 (70 %)

Table 4. Non-identified DSC peaks of different alloys in heating (above line) and cooling (under line)

Possible transformation	Temperature of phase transformation, °C	
	FS45	FS70
Peritectoid lebeauite + FeSi → β-$FeSi_2$	– 753	–
Peritectoid β-$FeSi_2$→ lebeauite + Si	–	909 –
Peritectoid β-$FeSi_2$ → lebeauite + FeSi	938 –	–
Caused by impurity phases	1151 –	–
Same	1255 –	–
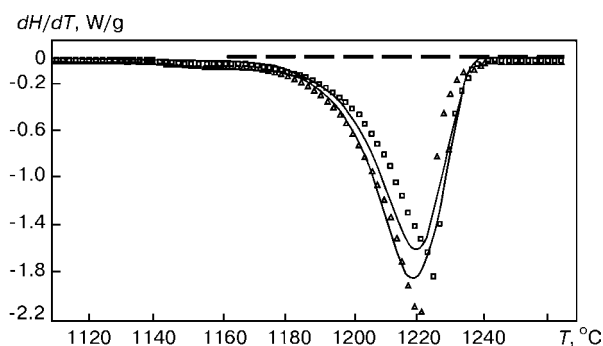
Figure 5. Kinetic curves of melting two samples of ferrosilicium FS45: signs — experimental data, lines — data of optimized model by Avrami–Erofeev equation

Figure 7. Change of enthalpy of ferrosilicium of FS70 grade depending on temperature

orders, processes controllable by diffusion and so on) (Figure 5). The highest correlation was obtained by two equations of Avrami–Erofeev [7], reflecting the processes of a volume nucleation in the formal theory of chemical kinetics:

$$\frac{d[A]}{d\tau} = F\, e^{-E/RT}\, n\, [A] \left\{ -\ln [A]\, \frac{n-1}{n} \right\},$$

where $[A] = A/A_0$ is the relative concentration of initial phase; n is the reaction order; F is the preexponential factor; E is the apparent energy of activation of eutectic reaction. The above-given expression for data of Figure 5 can be written in the form

$$\frac{d[A]}{d\tau} = 355\, e^{-13830}\, [A] \left\{ -\ln A \right\}$$

with 115 kJ/mol apparent energy of activation of melting process.

According the above procedure the specific heat capacity of alloy FS70 was calculated (Figure 6). Known heat capacity as a function of temperature makes it possible to calculate the enthalpy of alloy by integration (Figure 7). During analysis the change in enthalpy of alloy FS70 for independent reactions «liquidus-2», «eutectic-2» and «peritectoid β-FeSi₂ → lebeauite + Si» was determined. Here, the peaks of curve of heat capacity were classified by the Fraser–Suzuki [8] using the procedures of non-linear regression. In this method the signal is approximated by an asymmetric peak by equations:

$$y = A\, \exp\left[-\ln 2 \left(\frac{\ln\left\{ 1 + 2a\,(x - x_{\mathrm{r}})/W \right\}}{a} \right)^2 \right];$$

$$S = \frac{\sqrt{\pi}}{2\sqrt{\ln 2}}\, A \cdot W \exp\left[\frac{a^2}{4\ln 2} \right],$$

where y is the signal; A is the amplitude; W is the half-width of peak; S is the peak area; α is the peak asymmetry; x is the current coordinate; x_{r} is the peak position. It follows from the results of classification (Figure 8) that liquidus peak should spread to the region of sufficiently high temperatures (lower than 800 °C) that, probably, requires an additional explanation. Alloy FS70 contains a large amount of primary silicon (of about 30 % at 1210 °C), whose constant increase in heat capacity and decrease in share within the wide range of temperatures shift the base line of heat capacity towards the higher values. Therefore, numerical values of estimation of enthalpy of reactions refer to 1 g of alloy, but not to 1 mol:

Peak 1 «Peritectoid β-FeSi₂ → lebeauite + Si» $\quad \Delta H_1 = -30.6 \pm 13.5$ J/g

Peak 2 «Eutectic-2» $\quad \Delta H_2 = -247.0 \pm 8.4$ J/g

Peak 3 «Liquidus-2» $\quad \Delta H_3 = 504.5 \pm 19.1$ J/g

The above values of change in enthalpy are estimating, as the amount of primary silicon and impurities, which are «inert» as regards to reactions investigated is unknown a priori. At the same time it was established that the «eutectic-2» and «liquidus-2» transformations are accompanied by much higher changes in enthalpy than the peritectoid transformation of lebeauite. Difficulties in adequate determina-

Figure 6. Curves of differential scanning calorimetry and specific heat capacity in heating ferrosilicium of FS70 grade
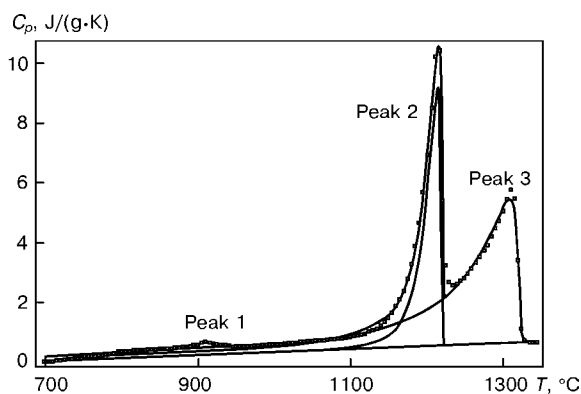
Figure 8. Classification and integrating of peaks of curve of specific heat capacity of ferrosilicium of FS70 grade

tion of the peritectoid transformation are, probably, associated both with a low heat effect of this reaction and also with a low rate of its proceeding. Indirect estimation shows that, assuming the change of enthalpy in melting silicon to be equal to 50206 J/mol and FeSi $\approx$ 75540 J/mol, the change of enthalpy of eutectic reaction will be 44000–47000 J/mol. If to consider that eutectic «lebeauite–silicon» is located very close to the phase region of lebeauite (Figure 1), then enthalpy of melting the latter in a commercial ferrosilicium will be 41440–42560 J/mol in principle.

The data obtained in this work are important for designing technology of pouring of ferrosilicium providing a high output of commercial classes of size in fractionation of ingots by crushing, sieving and also for thermal physical calculations of processes of dissolution of ferrosilicium of different grades in deoxidizing and alloying of steel or modifying of cast irons by silicon.

1. Gasik, M.I., Lyakishev, N.P. (1999) *Theory and technology of electrometallurgy of ferroalloys*. Moscow: Intermet Engineering.
2. (1997) *State diagrams of binary metal system*. Refer. Book. Ed. by N.P. Lyakishev. Moscow: Mashinostroenie.
3. Magnusson, Th., Sigfusson, Th., Helgason, O. (1998) Phase stability in silicon rich ferrosilicon. In: *Proc. of 8th Int. Ferroalloys Congress*, June 7–10, 1998, Beijing, China. Beijing: Ch. Sci.-Techn.
4. Sigfusson, Th., (1995) Ferrosilicon research in Iceland. In: *Proc. of INFACON'7*, June, 1995, Trondheim, Norway. Trondheim: FFF.
5. Zubov, V.L., Ovcharuk, A.N., Gasik, M.I. (2000) X-ray spectrometry examinations of microstructure of 45 % ferrosilicon produced by machine pouring. *Metallurgich. i Gornorudnaya Promyshlennost*, **4**, 33–34.
6. Gasik, M.I. (1996) Problems of scattering of high-percentage ferrosilicon accompanied with formation of toxic gases. *Stal*, **8**, 26–30.
7. Brown, M., Dollimar, D., Galvay, A. (1983) *Reactions of solids*. Moscow: Mir.
8. Selivanova, E.V., Stromberg, A.G., Romanenko, S.V. (2002) Modelling of asymmetric peaks in analytical chemistry — wire-frame model of asymmetric base peak of Koshi–Fraser–Suzuki. In: *Proc. of 2nd All-Russia Sci. Conf. on Chemistry and Chemical Technology at the Threshold of Milleniums*. Tomsk: TGU.

PROPERTIES OF ALLOYS
BASED ON HIGH-PURITY CHROMIUM

A.P. RUDOJ, V.Kh. MELNIK and **A.P. PORTNOV**

Institute for Problems of Materials Science, NASU, Kyiv, Ukraine

Chromium alloys, alloyed with lanthanum, iron, nickel and cobalt were produced from high-purity chromium ingots melted by induction-arc method. Hardness and transition temperature of these alloys were examined. It is shown that hardness decreased from 1350 to 1000 MPa, and temperature of brittleness decreased from 20 to −40 °C. It is also shown that alloy Cr−La−Fe is easily deformed by rolling and rotational forging. Ductility of this alloy makes it possible to produce the protective coatings from it. Tests of artillery barrels with this protective coating for gunpowder erosion showed the 3 times increase in service life of the barrels.

K e y   w o r d s: *chromium, alloy, hardness, brittleness temperature, processing ductility, protective coating*

Chromium, pertaining to metals of group VI of the periodic table, is highly sensitive to the presence of interstitial impurities (carbon, nitrogen, oxygen, hydrogen), which have a low solubility, wt.%: H — 0.00001−0.0001; C — 0.00001−0.0001; N — 0.00001; O — 0.00001. They form oversaturated solid solutions and two-phase alloys with chromium, this leading to impurity segregation on dislocations, which results in chromium proneness to intercrystalline fracture, and to lowering of low-temperature and processing ductility, respectively [1−3].

Since chromium has a number of useful properties and, in particular, high corrosion and erosion resistance in aggressive media, it is rational to use it as cathode material in coating deposition on the surface of items, exposed to aggressive media in service [4].

Chromium of ERKh grade (TU 14-5-3−65), produced by Russian companies, was used as initial material to melt out chromium ingots of 99.95 wt.% purity and up to 10 kg weight, by the technology of producing compact chromium, developed by us [5]. Chromium of a higher purity can be produced as small samples by iodide refining or other cleaning methods. However, during its remelting into larger ingots, chromium may be contaminated.

Protective coatings 50 to 60 μm thick, produced in vacuum by the method of ion-plasma spraying of high-purity chromium alloys, containing lanthanum (up to 0.3 wt.%), provided reliable protection of items from erosion damage in aggressive media at high temperatures. For instance, deposition of additional chromium coating on combustion chambers of liquid-fuel rocket engines, made of copper alloys with coatings of stainless steel and cobalt alloys, allowed improving the working temperatures of combustion chambers of jet engines and the power of the latter, respectively.

Attempts at protecting gun barrels, using coatings of high-purity chromium and its alloys with lanthanum did not yield any positive results, because of

coating cracking at impact loads and shots, which was, probably, due to formation of defects on dislocations.

Alloying of high-purity chromium, containing up to 0.3 wt.% lanthanum with metals of group VIII of periodic system, having atomic numbers, close to chromium and dissolving in it in the liquid and solid state up to 0.6 wt.%, enabled lowering HV hardness and brittleness temperature T_{br} of the produced three-component alloys.

Figure 1, *a* gives the dependencies of hardness of Cr−La−Fe, Cr−La−Ni and Cr−La−Co alloys on the content of alloying elements of iron, nickel and cobalt. It is seen that at small concentrations of the latter (up to 0.15−0.20 wt.%) alloy hardness is markedly decreased. With the increase of their concentration HV rises considerably, particularly so for alloys Cr−La−Ni and Cr−La−Co.

Investigation of the influence of alloying on brittleness temperature was conducted on the same alloys. T_{br} of initial alloys was close to zero. From Figure 1, *b* it is seen that at low concentrations of iron and nickel (up to 0.3 wt.%) brittleness temperature is lowered to −30 and −40 °C, respectively, and with the increase of their content T_{br} rises, which is indicative of a ductility drop. Cobalt definitely impairs the ductility of basic alloy Cr−La in the entire studied range of concentrations and, therefore, is not beneficial as an additive in development of a cathode alloy.

Thus, in view of the above, it may be assumed that nickel and iron have a favourable effect on the properties of alloys of Cr−La system, nickel additives increasing the ductility to a greater degree, and iron additives, contrarily, more markedly lowering the hardness of the studied alloys in as-cast condition.

The influence of annealing temperature T_{an} of cast alloys Cr−La−Fe and Cr−La−Ni, produced under our conditions, on their properties (HV and T_{br}) was also studied. Alloys of the following compositions were used, wt.%: Cr — balance; La — 0.11; Ni — 0.12 and Cr — balance; La — 0.22; Fe — 0.23. One-hour annealing was conducted in argon atmosphere in the

HV, MPa

*T*br, °C
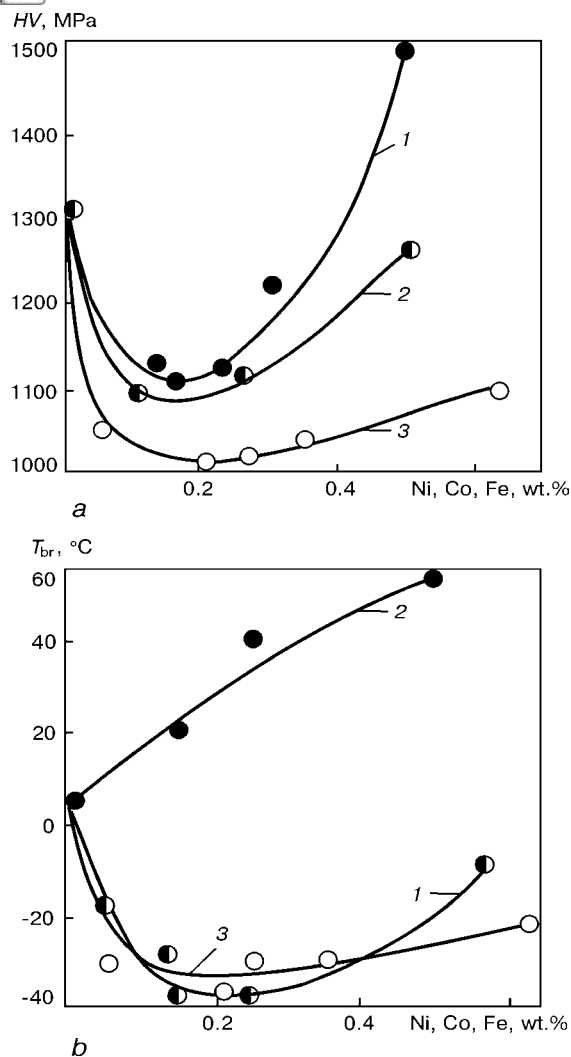
Figure 1. Influence of nickel (*1*), cobalt (*2*) and iron (*3*) on hardness (*a*) and brittleness temperature (*b*) of Cr–La alloys

HV, MPa

*T*br, °C

Figure 2. Influence of annealing temperature on hardness (*a*) and brittleness temperature (*b*) of Cr–La alloys, alloyed with nickel (*1*) and iron (*2*)

temperature range of 500 to 1000 °C. Alloy samples were cooled to room temperature with the furnace.

As is seen from Figure 2, *a* hardness of alloy Cr–La–Fe decreases smoothly up to annealing temperature of 900 °C, and then, at further increase of temperature, it rises markedly, which is attributable to redistribution of impurities between chromium and lanthanum. The nature of hardness variation with the increase of annealing temperature of Cr–La–Ni alloy follows the same law, but is not so pronounced.

Figure 2, *b* shows the variation of T_{br} with the increase of T_{an} of alloys Cr–La–Fe and Cr–La–Ni. If in the case of alloy Cr–La–Fe the nature of T_{br} dependence on annealing temperature, similar to that of *HV* on annealing temperature, is preserved, in alloy Cr–La–Ni a monotonic lowering of T_{br} is found with increase of annealing temperature in the studied tem-

perature range. Obtained data allow recommending one-hour annealing for cast alloys Cr–La–Fe and Cr–La–Ni to improve alloy ductility.

Results of the work performed by us showed the good prospects for application of low-alloyed chromium alloys of Cr–La–Fe and Cr–La–Ni systems as cathode material. At high processing ductility, allowing radial-type cathodes to be made of these alloys, they have a number of other advantages, namely good adhesion to item material, high-temperature resistance and cracking resistance. This was confirmed by conducted in Russia testing of gun barrels, the inner surface of which was coated by a protective layer of Cr–La–Fe, which demonstrated an increase of barrel life of about three times.

1. Trefilov, V.I., Firstov, S.A., Milman, Yu.V. (1975) *Basic physics of strength of refractory metals.* Kyiv: Naukova Dumka.
2. Gridnev, V.N., Trefilov, V.I. (1968) Studies on the problem of chrome. In: *Physical-chemical studies of refractory alloys.* Moscow: Nauka.
3. Trefilov, V.I., *Physical nature of metal brittle fracture.* Kyiv: Naukova Dumka.
4. Rudoj, A.P., Fialkovsky, R.V. (1976) Induction-arc process of fusion of metals. In: *Metal Phisics*, Issue 65.
5. Gridnev, V.N., Rozvorsky, A.M., Rudoj, A.P. et al. *Chrome-base alloy.* USSR author's cert. 751144, Int. Cl. C22C 27/06. Priority 15.06.78.

INDEX OF ARTICLES FOR ASEM'2002, No. 1–4